EUROPEAN FUSION DEVELOPMENT AGREEMENT
JET

EFDA–JET–PR(05)41

X. Litaudon

Internal Transport Barriers: Critical Physics Issues?

Internal Transport Barriers: Critical Physics Issues?

X. Litaudon

Association Euratom-CEA, DSM, Département de Recherches sur La Fusion Contrôlée, Centre d'Etudes de Cadarache, F-13108 Saint-Paul-Lez-Durance, France.

Preprint of Paper to be submitted for publication in
Plasma Physics and Controlled Fusion

ABSTRACT
Plasmas regimes with improved core energy confinement properties, i.e. with Internal Transport Barriers (ITB), provide a viable route towards simultaneously high fusion performance and continuous tokamak reactor operation in a non-inductive current drive state. High core confinement regimes should be made compatible with a dominant fraction of the plasma current self-generated (pressure-driven) by the bootstrap effect while operating at high normalised pressure and moderate current. Furthermore, ITB regimes with 'non-stiff' plasma core pressure break the link observed in standard inductive operation between fusion performances and plasma pressure at the edge, thus offering a new degree of freedom in the tokamak operational space. Prospects and critical issues for using plasmas with enhanced thermal core insulation as a basis for steady tokamak reactor operation are reviewed in the light of the encouraging experimental and modelling results obtained recently (typically in the last two years). An extensive set of data from experiments carried worldwide has been gathered on ITB regimes covering a wide range of parameters (q-profile, T_i/T_e, gradient length, shaping, normalised Larmor radius, collisionality, Mach number…). In the light of the progress made recently, the following critical physics issues relevant to the extrapolation of ITB regimes to next-step experiments, such ITER, are addressed:

(i) conditions for ITB formation and existence of a power threshold
(ii) ITB sustainment at T_i~T_e, with low toroidal torque injection at high density and low impurity concentration
(iii) control of confinement for sustaining wide ITBs that encompass a large volume at high β_N
(iv) real time profile control (q and pressure) with high bootstrap current and large fraction of alpha-heating
(v) compatibility of edge and core transport barriers

It is shown that the present experimental results provide some valuable and promising answers to these critical issues.

1. INTRODUCTION
This paper gives a review of the recent progress achieved in various tokamaks in view of developing regimes that could lead to efficient and purely non-inductive current drive tokamak operation with a large fraction of the plasma current self-generated (pressure driven) by the neo-classical 'bootstrap' effect. The analyses and discussion presented here focus on regimes usually achieved by controlling the current density profile leading to the formation of a core region with reduced anomalous radial transport (i.e; with improved core confinement) usually called Internal Transport Barrier, ITB. Regimes with ITBs have been extensively reviewed in the literature by [110, 68, 40, 37, 56, 115, 18 70, 15]. In addition to these past and comprehensive reviews, this paper draws attention to and discuss more in depth the critical physics issues that needed to be addressed for using plasmas with enhanced thermal core insulation as a robust basis for steady tokamak reactor operation. This proposed review is illustrated with examples taken from the encouraging experimental and modelling

progress obtained recently together with the results presented at 10^{th} IAEA Technical Meeting on H-mode and Transport Barriers (St Petersburg, 28 – 30 September 2005).

Steady-state operation in ITER is foreseen to be with 100% non-inductive current drive at reduced plasma current (I_p~9MA, q_{95}~5) with Q_{DT} the ratio of fusion power to input heating and current drive powers of the order of five, Q_{DT}~5, for a burning phase lasting up to 3000s [51, 3, 41, 99] Efficient steady-state operation should therefore be compatible with a large fraction (above 50%) of off-axis non-inductive current provided by the neoclassical bootstrap effect. The rest of the current is driven with externally applied non-inductive current drive in order to reach fully non-inductive state with zero loop voltage, V_{loop}, at the plasma boundary (no flux consumption). In this case, tokamak operation is foreseen with non-monotonic q-profiles characterised by a weak or a negative magnetic shear in the core of the plasmas. To compensate for the reduction of plasma confinement (due to operation at lower plasma current for optimising the bootstrap current), steady-state regimes require that the core confinement is improved beyond what it is achieved with an edge transport barrier alone. In comparison with present-day tokamaks, plasmas in next step devices, such as ITER, will be in a very different domain of dimensionless plasmas parameters that govern the transport properties with plasmas having a ratio of ion to electron temperature of the order of unity, T_i/T_e~1 and simultaneously low values of $\rho*$, $\nu*$, M_Φ [where $\rho*$ the normalised ion Larmor radius at the sound speed, $\nu*$ the normalised collisionality, and M_Φ the Mach number defined as the toroidal plasma rotation normalised to the sound speed] [51]. In this context, this paper presents a review and a discussion of the critical physics issues that need to be addressed in present day experiments in view of preparing these highly non-inductive integrated operations as foreseen in next step devices.

After this introduction, the paper is divided in three main parts. In section 2, the requests in terms of improved core confinement for steady-state fully non-inductive tokamak operation are discussed. It is argued that in order to fulfil both the requirements of bootstrap dominated steady-state plasmas and high thermonuclear fusion gain, it is necessary to operate at high values of normalised toroidal beta, β_N. In addition, it is shown that fully non-inductive current drive operation on ITER at Q_{DT}~5 will require improved core confinement with an enhancement factor in excess of the standard H-mode regime. In this context, regimes with Internal Transport Barriers offer a possible route to increase the core confinement and break the link between core and edge performances, thus offering a new degree of freedom in the tokamak operational space. Despite these promising aspects, it is recognised that ITBs in next step tokamak reactors will be formed and sustained in different operating conditions. This aspect raises the question of 'What are the critical physics issues relevant to a reliable extrapolation of ITB regimes to next-step experiments, such ITER, that need to be addressed in present day experiments or modelling activities?'. In section 3, this question is answered in more details where the recent experimental results (typically in the last two years) obtained in various tokamaks are reviewed in the context of the following issues:

(i) conditions for ITB formation and existence of a power threshold

(ii) ITB sustainment at $T_i \sim T_e$, with low toroidal torque injection at high density and low impurity concentration

(iii) control of confinement for sustaining wide ITBs that encompass a large volume at high β_N: control of ITB radial location and gradient strength

(iv) real time profile control (q and pressure) with high bootstrap current and large fraction of alpha-heating

(v) compatibility of edge and core transport barriers for achieving high confinement while respecting constrains imposed by plasma facing components

In section 3, it will be shown that the present experimental results and modelling effort provide some valuable and promising answers to these critical issues. Finally, in section 4 after a short summary of the recent progress relevant to these critical issues, a conclusion is given on the future activities where further experimental and modelling effort will provide valuable information required for a more reliable extrapolation of ITBs regimes in view of their application in next step devices

2. IMPROVED CORE CONFINEMENT FOR CONTINUOUS OPERATION

For continuous operation, all the plasma current must be driven by non-inductive means. It has been recognised that an efficient steady state thermonuclear tokamak reactor where the amount of re-circulating power for external current drive is minimised would need current drive efficiency which is practically an order of magnitude larger than presently achieved [90]. Therefore, development of efficient steady operation relies on the maximisation of plasma current self-generated (pressure driven) by the neo-classical 'bootstrap' effect [58, 61].

The fraction of the plasma current, Ip, driven by the bootstrap effect, I_{BS}, is given by

$$I_{BS}/I_p \propto \varepsilon^{1/2}\beta p \propto \varepsilon^{-1/2}\, q\, \beta_N \tag{1}$$

where ε is the tokamak inverse aspect ratio, the poloidal and toroidal beta parameters are respectively defined as $\beta_p = 2\mu_o \langle p\rangle/\beta_p{}^2$ and $\beta_t = 2\mu_o \langle p\rangle/\beta_p{}^2$ with $\langle p\rangle$ is the volume averaged total plasma pressure and B_p is the averaged poloidal magnetic field on the plasma surface. The normalised toroidal beta is defined as $\beta_N = \beta_t\,(I_p/aB_o)^{-1}$ (with β_t in [%], a the minor radius in meters, B_o the on-axis toroidal field in tesla and I_p the plasma current in megaamps) and q is the safety factor. It should be mentioned that the proportional factor between I_{boot}/I_p and $\varepsilon^{1/2}$ β_p is not constant and could be optimised depending on the plasma profiles and magnetic configuration (e.g. q-profile, existence of transport barriers, plasma shape etc). In a steady-state fusion reactor, maximisation of the bootstrap current fraction in the range of $I_{BS}/I_p \sim 70\text{-}80\%$ should be reached *simultaneously* with the optimisation of the fusion performance.

A measure of the fusion plasma performance is the power amplification factor, Q_{DT}. For stationary condition this is defined as the ratio of the fusion power produced to the additional heating power externally applied. Since the fusion power density is proportional to $\langle p\rangle^2 \propto \beta^2{}_t\, B^4{}_o$ (to about 10%

accuracy in the ion temperature range 10-20keV), the fusion gain, $Q_{DT,}$ in stationary conditions increases as :

$$Q_{DT} \propto \langle p \rangle \, \tau_E \propto \beta t \, \tau_E \, B^2{}_o \qquad (2)$$

where τ_E is the thermal energy confinement time. Therefore, optimising the fusion gain requires maximising simultaneously the energy confinement and β_t at high toroidal field.

In steady-state tokamak reactor, the fusion gain (β_t) and the bootstrap current fraction (β_p) have to be maximised *simultaneously*. The poloidal and toroidal beta are linked through this approximate relation [67]:

$$\beta t \, \beta p = 25 \, [(1 + \kappa^2)/2 \,] \, (\beta_N/100)^2 \qquad (3)$$

where κ is plasma elongation. Therefore, in order to fulfil both the requirements of continuous operation and high fusion gain, it is necessary to operate at high values of β_N and/or to increase the plasma elongation (in more general term the plasma non-circular shaping). This trade-off between fusion performance and steady-state operation is illustrated on figure 1 where β_t is plotted versus β_p (with $\kappa = 2$). The values of β_t and β_p are bounded by the low q operation and the high β_N MHD stability limits. The low q and high β_N limits are sketched in a schematic manner on Figure 1. In particular, the high β_N limit depends on plasma shaping, profile, (resistive) wall stabilisation and could be further optimised depending on the reactor design for steady-state operation. The conventional domain of inductive tokamak operation at q_{95}~3 (q_{95} is the safety factor value at 95% of the poloidal flux) is also indicated. In this standard tokamak operating mode, the fusion performance and the confinement are raised by increasing the plasma current (up to the low q limit) without optimising the bootstrap current fraction. In the other extreme limit (high β_p mode), the bootstrap current fraction is maximised by lowering the plasma current and operating at high q_{95} but at the expense of the fusion gain and fusion power density. The optimal route towards both high fusion gain and fully non-inductive current drive operation is obtained by increasing the β_N values, i.e. crossing the iso-β_N curves with an intermediate range of plasma current with q_{95}~4-5.

In this context steady-state operation in ITER is foreseen to be with 100% non-inductive current drive at moderate plasma current (I_p~9MA, q_{95}~5) with Q_{DT}~5 for a burning time of 3000s. Efficient steady-state operation should therefore be compatible with a large fraction of off-axis current provided by the neoclassical bootstrap effect, typically I_{BS}/I_p~50%. The rest of the current is driven with externally applied non-inductive current drive in order to reach full non-inductive current drive operation. In this case, operation with a non-monotonic q-profile is envisaged with a minimum q value, q_{min}, typically lying between 1.5 and 2.5 and with an absolute difference between the on axis q_o and q_{min} of the order of 0.5 ($|q_o - q_{min}|$~0.5) as proposed by the International Tokamak Physics Activity, ITPA, Steady-State Operation group. The typical range of q-profile for advanced operation is sketched in Figure 2. To compensate for the reduction of plasma confinement (due to operation at the lower plasma current for optimising the bootstrap current), steady-state operation requires the core confinement to be improved beyond that achieved with an edge transport barrier, with typically $H_{IPB98(y,2)} \geq 1.5$, $\beta_N \sim 3$ at $q_{95} \sim 5$.

This requirement in terms of improved core confinement has been further assessed for ITER using the CRONOS code in its 0-D version [6, 2]. The fusion gain, Q_{DT}, has been plotted on Figure 3 versus the enhanced confinement factor assuming ITER geometric parameters [41, 99]. The thermal ELMy H-mode confinement scaling law IPB98(y,2) [51] has been used in these calculations carried out with different density peaking factor, $n_{eo}/\langle n_e \rangle$, ranging between 1.1 and 1.7. In this set of curves the zero loop voltage condition is maintained when varying the H-factor and the plasma current is self-adjusted to the sum of the external and bootstrap non-inductive current. The heating and current drive schemes correspond to 33MW of Neutral Beam Injection, NBI, (at 1MeV energy), 20MW of Ion Cyclotron Resonance Heating, ICRH, power (55MHz 2^{nd} Harmonic of Tritium), and 20MW of Lower Hybrid Current Drive, LHCD (LHCD as a tool for advanced regimes as by reviewed by [112]. The Tritium fraction, $n_T/(n_D+n_T)$, is at the optimum value of 50% and the ratio of Helium retention time, τ^*_{He}, to thermal energy confinement time, τ_E is set to five. Whatever the density peaking factor, fully non-inductive current drive operation at β_N ranging between 2 and 3.5 will require $H_{IPB98(y,2)}$ in excess of 1.2, i.e. in the range of 1.2 and 1.8. In addition, control of confinement is essential during the fusion burn phase since Q_{DT} varies rapidly with a small change in confinement: at the nominal Q_{DT}=5 steady-state ITER operating point, ±10% variation of H-factor ($\Delta H_{IPB98(y,2)}/H_{IPB98(y,2)}$=±10%) could lead to a variation of ±50 % the estimated fusion gain ($\Delta Q_{DT}/Q_{DT}$ =±50%) at a density peaking of 1.5**.** The fusion gain increases strongly with the H-factor up to a saturation point (depending on the density peaking factor) where Helium ashes start to accumulate. On figure 3, saturation of performance is observed when the Helium density normalised to the volume averaged density, $n_{He}/\langle n_e \rangle$ exceeds typically 6% as indicated by a dashed line. Finally, it should be stressed that the calculations have been done using an electromagnetic energy confinement scaling law such as IPB98(y,2) with an unfavourable β scaling. This type of scaling law derived in inductive regimes needs to be validated at high values of β as obtained in advanced regime conditions. Therefore, calculation has also been repeated with a pure electrostatic and gyro-Bohm scaling laws [75, 85] with the lowest density peaking factor of 1.1. In this more favourable condition, an enhancement factor of 1.2 is still requires to reach a Q_{DT}~5 in fully non-inductive current drive conditions. To conclude on this analysis, continuous operation at constant flux on ITER at Q_{DT}~5 will require improved core confinement with an enhancement factor in excess of the standard H-mode regime.

In inductive operation with an edge transport barrier, the plasma temperature or pressure profiles are usually "stiff": when the temperature gradient exceeds a certain threshold, plasmas turbulence develops resulting in a large levels of anomalous radial transport which prevents a further increase of the local temperature gradient. Consequently, the pedestal temperature (at the top of the edge transport barrier) governs the global confinement properties and the fusion performances (c.f. figure

2 in [99] where Q_{DT} has been plotted against the pedestal ion temperature in ITER inductive conditions). High values of thermal confinement for steady operation will require to break the link between the pedestal pressure and the core confinement. This is indeed achieved in regimes with improved core confinement or internal transport barrier where the temperature profiles are not so strongly coupled to the boundary conditions. Using the recent JET database and following the approach proposed by Wolf et al [116], the core ion temperature has been plotted versus ion temperature measured at r/a~0.6 for various operating regimes with or without ITB on Figure 4(left). In regimes without ITB, the core temperature scales linearly with the boundary temperature as also found on ASDEX-U [82] and Figure 4 (right)) whereas in plasmas with ITBs this link is clearly broken on both devices. In addition, the normalised local temperature gradient, R/L_T where $L_T=T/\nabla T$, has been estimated at mid plasma radius using the JET database and compared to the expected theoretical scaling [52]. The result of this comparison is summarised on Figure 5. For both the ion (Fig.5 (left)) and electron (Fig.5 (right)) species, values of R/L_T in plasma regimes with ITB are well above the scaling for stiff profiles in clear contrast to the standard regimes with an edge transport barriers.

To conclude on this section, it has been shown that steady-state tokamak reactor requires operation at high β_N to simultaneously optimise the fusion performance and the self-generated bootstrap current. On ITER, full current drive operation with β_N in the range of 3 relies on achieving core confinement exceeding the values obtained in standard inductive regimes with uniquely an edge transport barrier. A promising route to reach this high confinement relies on optimising the core confinement, i.e. combining an edge transport barrier with an internal one. With ITB plasmas, it has been illustrated with the present experimental database that the link between the edge and core temperature is broken. This extra degree of freedom allows to increase the confinement factor and the bootstrap current fraction without uniquely increasing the pressure at the edge pedestal.

3. CRITICAL PHYSICS ISSUES FOR CONTINUOUS OPERATION WITH INTERNAL TRANSPORT BARRIERS

After having discussed, in the previous section, the necessary requirements for optimising the core confinement in view of steady tokamak reactor operation, the critical physics issues for using plasmas with enhanced thermal core insulation are then reviewed in the light of the encouraging experimental and modelling results obtained recently.

3.1 ITB BIFURCATION AND POWER THRESHOLD

An important issue is first to assess the conditions for triggering ITBs and to characterise the transition that leads to a change in the nature of the plasma turbulence. As reviewed by [18], the concept of phase transition can be locally applied to ITB formation where the local heat flux, Γ, is driven by the plasma temperature gradient, ∇T [65]. As shown on Fig.6 (left), the transition could occur at a critical value of the heat flux and displays hysteresis process for the back transition (‘first order’ transition). The second way is illustrated on Fig.6 (right) in which the bifurcation appears as a smoother transition ('second-order' transition) without a discontinuity of ∇T. For this latter type of transition, the ITB could be interpreted either as a regime with a higher degree of 'stiffness' (case 1 in Fig.5 (right)) or below the threshold for triggering anomalous transport (case 2 in fig. 5 (right)) as discussed in [73]. In order to illuminate the nature of the transition, pertubative techniques such cold pulse propagation or power modulation to vary the heat source are required [73], [79].

Experiments have been performed in JET, where the electron heat flux has been modulated using the ICRH power in a mode conversion scheme into an electrostatic Bernstein wave (for direct electron heating) in an ITB plasmas triggered and sustained in a magnetic configuration with non-monotonic q-profile (negative central magnetic shear) as reported by [73]. The recent and comprehensive analyses of these experiments, indicate that the ITB behaves as a narrow layer (less than 0.2 in normalised radius) of reduced heat diffusivity and favour the interpretation of ITB formation in terms of a second-order transition process with a loss of "stiffness" as sketched in case 2 of Figure 6 (right).

On JT-60U [61], dependence of the thermal heat diffusivity on the heat flux has been investigated by systematically varying the neutral beam power for both positive and negative magnetic shear configuration (Figure 7) [94]. The conclusions drawn from these experiments depend on the selected magnetic configuration (q-profile). In the case of positive magnetic shear plasmas, the thermal transport coefficients (χ_e and χ_i) in the core region first increase with the heating power as in standard L-mode regime, i.e. the so-called 'power degradation'. Then, above a certain threshold in power (~3MW of NBI power) weak ITB is formed and χ-values start to decrease. This behaviour could be reminiscent of a first-order type of transition. In the case of negative magnetic shear plasmas, no power degradation is observed and the χ-values decrease continuously with the applied heating power as it could be expected for a second-order type of transition. In this case it is difficult to define a threshold power since it is very small even suggesting the absence of any threshold provided that the magnetic configuration (q-profile) is properly optimised. Practically, the 'threshold' condition will be the non-inductive current drive sources to form and sustain the non-monotonic q-profile whereas the core-heating will be required to illuminate and control the region with improved confinement.

The experimental results that have been presented in this sub-section, address the general question of the power threshold for ITB formation. The simplified zero-dimensional (0-D) approach using global engineering variables, seems not to be sufficient to correctly answer to the difficult question of the conditions for ITB formation at a given radius and gradient strength. In particular, it has been seen that the magnetic topology plays an essential role in the ITB formation and could possibly change the nature of the transition. One should include in the power threshold consideration relevant information on the q-profile as the exact value of the local magnetic shear and the proximity to rational q-surfaces [62, 47, 31, 14, 88, 24, 53, 4, 79, 33 1, 87]. The importance of the zero magnetic shear surface should also be treated correctly: do we have a smooth effect or a threshold condition when the magnetic shear is reduced down to zero? [32, 12, 45]. In addition, a combination of magnetic shear stabilization and **E×B** shear flow (here **E** is the radial electric field and **B** the equilibrium magnetic field) [11] are important factors in explaining the ITB formation and should be included in a power threshold scaling law.

The complementary approach consists in developing and benchmarking comprehensive transport codes based either on empirical scaling or theory-based model [81, 59, 106, 107, 38, 9, 10, 44, 107]. Activity consisting in benchmarking transport models on various devices using experimental scans in q-profile, **E×B** shearing rate and β (α-stabilisation) are of prime importance in order to determine the relative role of these turbulence stabilisation mechanisms in the triggering and sustainment of ITBs. On JET, the 1-D first principle transport Weiland model [114] could satisfactorily reproduce the time dynamics, location and strength of the ITBs only in the case the experimental poloidal rotation is used instead of the neo-classical value [108]. It was indeed found on JET, from recent measurements of the poloidal rotation across ITBs, that the velocities are typically an order of magnitude higher than the neo-classical predictions and this leads to a quantitative difference in the evaluation of the radial electric field and **E×B** shear flow[19]. Recently, [10] have compared Gyrokinetic simulations (using the GYRO code) with measurements of transport and density fluctuations in a JT-60U plasma with strong ITBs (so called box-like). The reduction on JT-60U of the density correlation length down to the order of the ion gyroradius inside the ITB as reported by [77] was found to be comparable with the predicted one using gyrokinetic simulations [10]. ITBs formation have been modeled using empirical scaling laws found on JT-60U for the ITB width that is proportional to the ion poloidal gyroradius and for the thermal energy inside the volume limited by the ITBs radius [44]. Finally, using data from the profile multi-machine database, [38] have assessed various predictive transport models by comparing a pair of discharges from DIII-D, JET and JT-60U with respectively monotonic or non-monotonic safety factor profiles. Comprehensive tests of the transport models on various devices (with different sizes and operating conditions) are crucial and they have indicated that improvements in the treatment of the transport suppression mechanisms are required in order to enhance their predictive capability [38].

In this context, dimensionless identity and similarity experiments between different experimental devices should be carried out since it could reveal the size scaling of the conditions for ITB formation. Recently, identity experiments have been carried out between ASDEX Upgrade and JET, showing similar ITB phenomenology when matching the normalised physics quantities in the two devices [16, 113]. The parameters for the two experiments were matched as close as possible, using similar plasma shape and monotonic q-profiles (with $q_0 \sim 2$) together with closely matched values of ρ^*, ν^* and β just prior to the ITB formation phase (c.f. Table 1 and Figure 8). In addition, comparable power deposition profiles with neutral beam heating has been applied in the current ramp-up phase. In these conditions, ITBs have been formed in both machines at a power level of 7-10MW on the ion species but electron ITBs have not been observed. Both experiments did report transient ITBs, which collapsed with the onset of large ELMs (Figure 8 (right)) (ELMs mitigation techniques by impurity injection were then developed on JET to sustain ITBs on a longer duration). This preliminary set of experiments opens a new field of research in the ITB regime which should grow in importance in the coming years since these regimes enter in a more mature and reproducible phase in most of the experimental devices after the initial development phase in the years 1990. This is of prime importance for increased understanding of the ITB bifurcation process and a reliable extrapolation of the ITB regimes to devices with different size such as ITER.

3.2 ITB AT TI~TE, WITH LOW TORQUE INJECTION AT HIGH DENSITY AND LOW IMPURITY CONCENTRATION

Another important issue when extrapolating the advanced regimes towards next step experiments, is the possibility of forming and sustaining these modes of operation with reduced toroidal rotation, V_ϕ, and with a ratio of ion to electron temperature around unity at high density. In the context of alpha particle heated plasmas, the fusion born fast alpha particles will heat predominantly the thermal electrons, which in turn will heat the ion species through collisional energy transfer resulting in a regime with T_e~T_i at high plasma density where electrons and ions are strongly coupled.

The answer to this important question of the formation and sustainment of ITBs with T_e~T_i seems once again depends on the shape of the current density profile. On the one hand, in negative central magnetic shear configurations, ITBs have been sustained with T_e~T_i on ASDEX-U [43, 49] by combining Neutral Beam Heating with Electron Cyclotron Resonance Heating, and on JET [113] with similar NBI and ICRH heating power levels in pellet fuelled ITB reaching at core density up to $6\times10^{19}m^{-3}$. On JT-60U in negative magnetic shear ITBs regime, the improved confinement factors have been plotted against the ratio of T_e/T_i and the observed trend does not indicate any degradation of confinement when operating at $T_e/T_i \geq 1$ as illustrated in Figure 9. On the other hand, degradation of ITBs performance is observed in the ion temperature and toroidal rotation profiles in monotonic q-profile with positive magnetic shear on JT-60U [49, 96] and on DIII-D [13] when ECRH is added in NBI heated discharges. This degradation of the ion ITB has been interpreted recently by [13] by calculating the critical ion temperature gradient for triggering ITG turbulence that strongly depends on the ratio of T_e/T_i. Prior to the ECRH application, the normalised ion temperature gradient R/L_{Ti} is below the critical value for triggering ITG turbulence consistent with the sustainment of ion ITB. When increasing the T_e/T_i ratio with ECRH, the critical ion temperature gradient for ITG turbulence is reduced and becomes comparable to the measured R/L_{Ti} that leads to a reduction of T_i driven by the increase of turbulence level. In addition, this effect has an unfavourable feedback loop, since the reduction of T_i leads to a further increase of T_e/T_i that in turn reduces the critical ion temperature gradient.

In most of the high fusion performance ITB regimes, low energy neutral beam injection is used to provide most of the heating power that dominantly heats the thermal ions species and generates high plasma rotation. Large toroidal rotation and associated Mach number, M_ϕ, induced by neutral beam injection at T_i/T_e>1 may facilitate the transition and sustainement to high confinement regime (e.g. toroidal rotation term in the ExB shearing stabilisation, T_i/T_e dependence on linear growth rates as previously discussed). Such mechanisms might not be sufficient in ITER plasmas heated with high energy neutral beam (E_{beam}~1MeV) since the injected NB torque scales as $(1/E_{beam})^{1/2}$. The typical range of averaged toroidal rotation that could be reached in ITER steady-state has been estimated at V_ϕ ~100-150km/s, corresponding to M_ϕ ~0.2[1] that is much lower than the values obtained in the present high performance experiments. The possibility of varying the NBI injected torque has been first reported on TFTR [104] and on JT-60U [100, 56]. On JT-60U, more favourable ITBs sustainement conditions have been reported with balanced NB injection thanks to a local notch of the toroidal rotation (large and radially localised variation of the toroidal rotation) at the ITB location that leads to high values of E×B shearing rate [100]. In the next experimental campaign DIII-D, will also have the possibility to vary the injected torque and address this important issue since two out seven NBI injectors will be re-oriented in counter-current direction. On JET, a new ICRH antenna will be installed and should provide a further increase of the coupled power without increasing the injected torque. For addressing this issue, an important class of experiments where ITBs have been successfully formed with low torque injection represent the ones that uses mainly Radio-Frequency heating schemes. Such experiments have been reported in Alcator-C [91, 28], DIII-D [42], FT-U [83], JET [47, JT-60U [30, TCV [98. 26] and Tore Supra [46, 84, 69 by using ICRH or/and ECRH or/and LHCD powers. Due to a limited available RF power, these experiments are usually performed at a lower level of fusion performance compared to the NBI heated cases but they provide significant information on the ITB physics with low torque injection. The general trend usually reported is that ITBs are triggered mainly by negative magnetic shear effect and then it could be sustained depending on the heating power by a combination of magnetic shear and ExB shear stabilising effect if the barrier is fully developed [46]. On TCV, O. [98] have clearly shown that electron ITBs could be controlled by only modifying the current density profile at constant input power and without momentum input. A fine control of the current density profile has been obtained by systematically introducing either a positive or negative on axis ohmic current perturbation by varying the applied loop voltage around the fully non-inductive current drive state (in these experiments, the ohmic transformer was set to control the poloidal flux rather than the total plasma current). As indicated in Figure 10, a continuous increase of the electron transport barrier strength (and therefore of global electron confinement) is reported when the current profile was varied from a monotonic to a non-monotonic one. It is also concluded, that a negative magnetic shear configuration is required to significantly enhance the global confinement above unity. These experiments pave the way towards a control of the electron confinement by tailoring (and ultimately in real time) the q-profile. Finally, it should be stressed that these RF regimes are mainly associated with the formation of an electron ITB and it is still an issue of debate and experimental investigation to determine whether ITB on V_ϕ, T_i and density profiles could be formed and sustained with low torque injection.

Access to high density ITB is an important issue to be addressed in present day experiments since advanced tokamak regimes on ITER should be performed typically at a density of ~$7\times10^{19}m^{-3}$

[1]The averaged plasma toroidal rotation is deduced from th injected NB torque and the (0-D) conservation equation of the global angular momentum. It is assumed that the toroidal angular momentum confinement time is equal to the energy confinement time deduced from the empirical scaling laws (IPB98(y,2)).

corresponding to a density normalised to the Greenwald density, n_G, of 0.8 and simultaneously at low normalised collisionality ($\nu_e* \sim 2\times10^{-2}$) due to the high expected electron temperature. Studies of the particle transport inside ITBs plasmas is a relatively unexplored area of research. Recently on JET, tritium transport coefficients deduced from pertubative trace tritium experiments are seen to approach neo-classical levels in the plasma core inside the ITBs [118]. In electron ITB regimes formed on TCV, it has been reported from recent studies that local electron density gradients are well correlated with the gradients of the electron temperature inside the core improved electron confinement region [26]**.** In present day experiments, AT regimes could not be performed simultaneously at high density, low collisionality and high normalised Greenwald density but these parameters could be studied independently. High confinement ITB regimes are usually obtained at reduced density that approaches the expected ITER collisionality regime as shown in Figure 3 in [70] using multi-machine data from the ITPA global database. At n/n_G~0.8-1 and at $n\sim7\times10^{19}m^{-3}$, improved confinement factor are below 2 and it has been observed that high triangularity configuration is more favourable to reach high confinement at high density. The difficulties in simultaneously reaching high densities with good core confinement in the advanced regimes could be understood as follows. When increasing the density, the flexibility to form and sustain the optimised current density profile for confinement and stability is reduced: (i) faster resistive inwards diffusion (lower temperature) of the transient off-axis ohmic current induced during the current ramp-up phase of the discharge and (ii) lower level of non-inductively driven current by external means. Furthermore, the induced plasma rotation that has the potentiality to reduce the plasma turbulence through velocity shear is expected to be lower at higher density. Therefore, an important objective for future advanced tokamak experiments is to develop a route towards high confinement at high density and progress has been made recently on this field. On FT-U, electron ITBs with high confinement properties have been recently sustained during one resistive current diffusion time (~18 confinement time) with a combination of LHCD and ECRH heating at a core density well in excess of $10^{20}m^{-3}$ at n_l/n_G~0.5 and high collisionality [83]. On JT-60U, reversed shear ITBs have been sustained at n_l/n_G~1 with a high enhanced confinement factor ($H_{IPB98(y,2)}$~1.2) but at a density of $3.5\times10^{19}m^{-3}$ since the plasma current was reduced down to 1.0MA (q_{95}~6.1) [104]. On JET, ITB at high density (n_{el}/n_G~0.85) with steep gradients in the density profile has been formed transiently with respect to the current diffusion time scale (4-6 times the energy confinement time) with pellet fuelling in negative magnetic shear configuration [29, 113].

High density ITB operation is required in particular for increasing the fusion performance and the bootstrap current but this should not be obtained at the expense of core impurity accumulation in particular of medium and high-Z elements. Indeed, such materials might be used for sustaining high heat load on some of the plasma facing components (like Tungsten coating on the divertor plates) and also for impurity seeding (like Argon) to control the edge radiated power. The quantitative studies of the impurity transport in strong ITB plasmas have shown that the impurity behaviour could follow the trends predicted by the neo-classical theory: high Z-impurity accumulation with strong peaking of the density profile competing with the screening effect expected from high ion temperature gradient [105, 23]. A core radiative collapse could even be observed when the temperature screening effect is either too localised and/or not strong enough to prevent the central accumulation of the high-Z impurity [23, 71]. To avoid the deleterious impurity accumulation effects, density gradient of the main ion should be controlled so that the inwardly directed convective fluxes driven by ∇n become smaller than the outwards drift velocity driven by ∇T_i. For a given value of ∇T_i the neoclassical expression of the radial drift velocity ($v_{neo} \propto \nabla n_D/n_D - \alpha\ \nabla T_i/T_i$) should set a maximum value of density gradient that should not be exceeded to avoid impurity accumulation. For a flat plasma density profiles, recent simulations of impurity transport for ITER scenarios have shown that the neoclassical temperature screening effect successfully assists in removing high-Z impurities from the plasma core in reversed shear ITBs regimes [66]. On the experimental side, density gradients have been controlled in indirect manner on ASDEX-U [78], DIII-D [13], JT-60U [105], by applying on axis electron heating. These techniques usually rely on an increase of the core turbulent transport to raise the ion heat and/or particle diffusivities. For the low Z-impurities, the key question is the control of the helium 'ash' since a too high level concentration of core ashes will affect the fusion performance in the D-T burn phase in ITER (c.f. Figure 3) and in fusion tokamak reactors. On JET, the ratio of the Helium retention time to the thermal energy confinement time is found to be in the range of 5-8 for quasi steady-state ITBs and Helium could be effectively pumped [118]. In the JET experiments performed with weak ITBs in negative magnetic shear configuration the global confinement was not dominated by the core conditions and therefore Helium transport experiments should also be repeated in high fusion performance conditions with high core plasma pressure (beta). On JT-60U, promising results have been found indicating that Helium (and Carbon) is not accumulated inside the ITB even with ion transport close to a neoclassical level [105].

3.3 CONTROL OF CONFINEMENT FOR SUSTAINING ITB AT HIGH β_N: CONTROL OF ITB LOCATION AND STRENGTH

Sustainment of high fusion performance ITB plasmas will need a simultaneous control of the ITB radial location, strength and width since an optimal class of kinetic profiles is indeed required [21, 72]. Pressure profiles representing in a schematic way different cases of ITB profiles (optimal and non-optimal ITB profiles) at constant volume averaged pressure are illustrated on Fig.11. The optimal ITB profiles lie at a large radius, possess moderate gradient and encompass a large region with improved confinement (large ITB width). For the same global energy confinement and volume averaged pressure, optimal ITB profiles have the merit of :

(i) increasing the MHD stability limit to access to high β_N operation [72]; ideal pressure driven kink modes with highly peaked pressure profiles (narrow ITBs case) could be destabilised at very low values of β_N (below 2);
(ii) optimising the bootstrap current profile that locally depends on the various gradients of the kinetic profiles; this in view of driving a broad bootstrap current density profile consistent

with the requirement of a broad total current density profile (c.f. figure 2 for the current profile requirement); On the contrary, a too localised bootstrap current generated in the narrow ITBs case could lead to the formation of 'current hole' magnetic configuration with vanishing on-axis current [15];

(iii) reducing the core impurity accumulation with a broad density profile as discussed in the previous section.

Figures 12 summarises the normalised performances achieved so far in advanced regimes in an operational diagram using the multi-machine ITPA global database where β_N values have been plotted against pressure peaking factor [107, 70]. The data confirms that a broad pressure profile is favourable for raising β_N. This is consistent with the ideal pressure driven kink modes that are destabilised with highly peaked pressure profiles. In order to broaden the pressure profiles for stability reasons, it is necessary to develop wide ITBs regimes combined with an edge transport barrier. Recently DIII-D has developed ITBs discharges with broad pressure and current profiles at high q_{min} ~2 [72, 34]. The broad current profile was obtained by simultaneously ramping down the toroidal field and ramping-up the plasma current to rapidly reduce q_{95} (~5.5-3.5) without affecting too much the central part of the q-profile in the hot core region heated with NBI power and ECRH. Broad ITBs clearly observed on the toroidal rotation, ion temperature and density profiles have been sustained during 2s (τ_E~0.16s) at β_N ~4 with a pressure peaking factor in the range of 2.5-3.2. Resistive wall mode stabilisation was found to be essential to these plasmas which did perform at β_N values above 6 times the internal inductance. Despite that these results have been achieved with non-stationary q-profiles, they clearly indicate the existence of a favourable route where pressure and q-profile could be optimised to sustain ITBs plasmas at high β_N values.

The possible approach to control the core confinement in view of reaching the optimal class of ITB profiles (Figure 11) could be summarized as follow:

(1) control of the density gradients; it is well known that large density gradient (e.g.. induced with core pellet fuelling) could stabilize the ITG turbulence but this approach is in contradiction with the request of broad density profile for avoiding impurity accumulation;

(2) control of the T_i/T_e ratio; by increasing this ratio the critical gradient for ITG threshold could be increased but contrary to most present day experiments operation on ITER is foreseen at T_i/T_e ~1;

(3) impurity injection; DIII-D [20]and JET have reported ITB expansion by injecting a controlled quantities of impurities but this approach has a limited prospect since core impurity accumulation should be avoided.

(4) E×B flow shear stabilization; the rotational term in the E×B shearing rate γ_{ExB}, has been varied in present day experiment with various NBI power level and also with different ratio of co- to counter current injection. On JT-60U [93], DIII-D [21] and MAST [27] have concluded that control of the toroidal rotation could be favorable for ITB expansion when (for example in counter-injection cases) the diamagnetic and the toroidal terms in the ExB shearing rate expression add-up. On ITER, the control of rotation will be limited with high energy NBI (co-injection); therefore one should rely on the control of the diamagnetic and poloidal terms in the ExB shearing rate expression; these two terms have an unfavorable scaling with ρ^* ($\gamma_{ExB}/\gamma_{ITG} \propto \rho^*$) but a positive feedback loop between the ExB shearing and the pressure could reinforce their contribution.

(5) ***α-stabilization*** ($\boldsymbol{\alpha \propto -q^2\beta R\nabla P/P}$)***;*** high values of the α parameters could reduce the curvature and ∇B-drift driving curvature type of micro-instabilities (as low or negative magnetic shear) [8]. This stabilization mechanism scales in favorable manner with increasing β (and q) without an unfavorable size effect and does not require momentum injection. As discussed recently in [9] when analysing ITBs experiments from the ITPA multi-machine profile database, ITBs could be self-sustained in certain conditions thanks to a positive feedback loop between pressure and the α stabilising parameters.

(6) ***q-profile;*** reduction of the local magnetic shear could decrease the plasma turbulence in particular close to low order rational q-surface. Off axis non-inductive current drives has been successfully used to tailor the q-profile in present day experiments. For instance, it has been shown in JET by [106] that the level of ExB shearing rate to form and sustain wide ITB at large radius will be lower by decreasing locally the magnetic shear. In addition, there is an attractive positive feedback loop between the magnetic shear and the off-axis bootstrap current self-driven by the pressure gradient that reduces the magnetic shear at the ITBs location [5] For these reasons, q-profile control (further discussed in the next sub-section) is a particularly promising way of affecting the core confinement and provides a route to sustain wide ITBs in future burning plasmas experiments like ITER.

3.4 REAL TIME PROFILE CONTROL WITH HIGH BOOTSTRAP CURRENT AND LARGE FRACTION OF ALPHA-HEATING

Reliable steady-state operation will require a simultaneous control of the various kinetic and current density profiles under the conditions of a highly autonomous state. This is a challenging task because of the strong (non-linear) coupling of the q-profile, thermal confinement, bootstrap current, fusion power and MHD stability. MHD stability analysis against ideal mode of the steady-state operation on ITER with broad or weakly negative shear q-profile has indicated a clear requirement in terms of q-profile control and its minimum value [99, 86]. It was numerically found, that at the ITER wall position (a_{wall}/a=1.375 with a =1.85m), the marginal β_N is 2.6 for a minimum q value of 2.1 and 3.85 for q_{min}=2.4.

The requirements in terms of profile control has been also stressed recently by recent observations of oscillations in confinement when reaching fully non-inductive current drive regimes on Tore Supra mainly sustained with LH waves [35, 36, 50] and in DIII-D in dominated bootstrap conditions [87]. During constant flux operation on Tore Supra, the most plausible explanation of the steady oscillation invokes the non-linear coupling between the current density and the electron temperature

[35]: the LH non-inductive current depends on the electron temperature and q-profile whereas the electron confinement depends on the current profile. When a low magnetic shear configuration is reached the electron thermal confinement locally improves (T_e increases) and the on-axis part of the LH current grows that leads to a decrease of the central q values (monotonic q-profile), resulting in a reduction of both T_e and the on-axis part of the LH current, then the cycle could restart. More recently, it has even been observed that this sinusoidal oscillations phenomenon could be accompanied by phases of giant oscillations ($\Delta T_{eo}/T_{eo}$~50%) as shown on Figure 13 (left) so that the Tore Supra plasmas behave as two-cycles non-linear oscillators [50, 36]. The onset of giant oscillation in core electron temperature is thought to involve, in addition to the previously described mechanisms, MHD activity that is triggered when the q_{min} value approaches a low order rational q-surface (q_{min} ~2). Similarly on T-10, in ECRH heated plasmas it has been observed that if the q-profile is still evolving the ITBs are destroyed and then immediately reformed when q_{min} values cross low order rational q-surfaces [60]. On DIII-D (Figure 13 (right)), relaxation oscillation of confinement ($\Delta W/W$~50%) and plasma current is observed in non-inductive current drive regime with a dominant fraction of bootstrap current where the transformer flux is set to control a zero loop voltage at the plasma boundary as on Tore Supra or TCV [87]. The process occurring in these plasmas is the repetitive build-up and collapse of an ITB at large minor radius: this is at present the limiting process for beta and bootstrap current in these operational conditions. Characteristically these plasmas have a dominant fraction of bootstrap current in the range of 65-85%, maintained for up to 3.7s at $\beta_N \sim \beta_p$ approaching 3.3. A possible explanation of this oscillating phenomenon could be found in the coupling of the total current profile, thermal confinement (kinetic profiles) and bootstrap current.

An important experimental programme is in progress in many devices (e.g. DIII-D, JET, JT-60U, Tore Supra) to investigate real time plasma profile (kinetic and magnetic) control schemes which could be applicable to achieve reliable steady state regime on ITER. On DIII-D, active feedback (closed loop) control of the q-profile (either q_o or q_{min}) evolution has been performed during the initial plasma formation using either ECRH or NBI power for the control actuators (with simplified proportional gain) acting on the conductivity profile (Gohil et al 2005). Figure 14 (left) is an illustration of the control of q_o with off-axis ECRH power achieved in L-mode discharges on DIII-D by altering the ohmic current penetration rate through changes in T_e and hence in conductivity [40].‘In a similar manner, NBI has been used for feedback control of‘q_{min} in H-mode plasmas at β_N reaching up to 2.5 [39]. On JT-60U [103], q-on axis has been controlled with Lower Hybrid waves by varying in real time the injected slow-wave spectrum in view of changing the off-axis LH current location. On JET initial experiments where the ITB strength was controlled with ICRH power did indicate that the current density profile was slowly evolving leading to an uncontrolled ITB position [74]. Consequently, multi-variable model based technique has been developed for the simultaneous control of current and temperature profiles in ITB discharges using LHCD together with NBI and ICRH [76, 63, 108]. The control scheme relies on the experimental determination of a linearised integral operator between the actuactors and the plasma profiles. The first experiments using this technique have already indicated that different current and electron temperature profiles can be obtained and sustained by the advanced controller in closed loop operation [63] Figure 14 (right) shows such successful control when a non-monotonic target q-profile was requested with a normalised electron temperature gradient just exceeding the threshold value set by the ITB criterion defined by [111].

A important development remains to apply these real time control techniques in conditions where the bootstrap current is the dominant non-inductive current drive source. The progress in sustaining high bootstrap regimes is summarised on Figure 15 using the data from the multi-machine ITB database. In TCV [17], using ECRH system to control (not in real time) the current and temperature profiles, fully non-inductive steady-state electron ITBs have been sustained (up 5 times the resistive current diffusion time, τ_R) with a bootstrap current fraction up to 75% (β_p~2.4) without any sign of plasma internal relaxation as observed on DIII-D [87]. On JT-60U, a large bootstrap current fraction (up to 75%) has been sustained for 7.4s (~$12\times\tau_E$ corresponding to ~$2.7\times\tau_R$) in a negative magnetic shear configuration and this duration was only limited by the duration of the neutral beam injection [95]. The key ingredient in this recent progress since previously reported results [30], was the control of the pressure gradient and rotation at the ITB by combining co with counter NBI injection in order to avoid a plasma disruption when q_{min} did evolve across integer values. Direct q-profile control might also be valuable to slow down the q-profile evolution.

These bootstrap dominated regimes have been sustained at reduced plasma current and high q_{95} values (well above 5): i.e. at the expense of the actual fusion performance, since they are usually limited in power. On JET, by increasing the power and current drive capability to ~45MW, 0-D calculation indicates that the operational space of the advanced tokamak regime could be extended dramatically in terms of current (>2.5MA) and density ($n_l>6\times10^{19}m^{-3}$) with high β_N (β_N~3.4) and a bootstrap current fraction in the range of 70% at high toroidal field (~3.5T). On Figure 16, the calculated fusion triple product is plotted against the bootstrap current fraction for various power level in fully non-inductive current drive conditions combining LHCD, Neutral Beam Current Drive with ICRH heating (assuming that confinement scales as the ELMy H-mode, but with a confinement enhancement factor increasing with power as observed in the present JET ITB database). A power level of 45MW gives access a regime where, as in a future steady-state reactor, the bootstrap current is maximised together with the fusion yield and not at the expense of fusion yield as in present day experiments (i.e. by lowering the plasma current and/or toroidal field).

The ultimate challenge will be to develop real time control techniques in high bootstrap regimes but also in conditions where the alpha-particle heating source could already be simulated experimentally using for instance on-axis ICRH heating as it was done in standard ELMy H-mode regimes [54]. Indeed, in future burning plasmas reactors the dominant heating source is the internal alpha-heating which strongly depends on the plasma parameters. This is an open field of research and further progress (experimental and modelling) is indeed required to design the most reactor relevant control techniques for burning plasmas conditions that minimise the requirements in term of external heating powers.

3.5 COMPATIBILITY OF INTERNAL WITH EDGE TRANSPORT BARRIER

As reviewed by [37], the combination of internal with edge transport barrier, H-mode edge, (ETB) is advantageous since it can lead to:

(i) higher fusion performance with better confinement properties at high beta;

(ii) broader pressure profile with improved MHD stability against destabilizing n=1 modes (as also discussed in sub-section 3.3) providing a route towards high β_N operation ;

(iii) a higher fraction of bootstrap current thanks to edge pressure gradient by naturally increasing the off-axis non-inductive current driven outside the ITB; off-axis current outside the ITB is indeed required to maintain broad current density profiles.

A critical issue is the compatibility of ITBs at large radius with a strong edge pedestal in particular with edge MHD perturbations such as ELMs activity. On ASDEX-U, DIII-D, JET, it has been frequently reported that large amplitude Type I ELMs could lead to an erosion or even a collapse of the ITBs that triggers back transition to a state with lower core confinement as reviewed in [37, 7, 97]. Figure 17 illustrates with a JET example the lost of the hot core ITB phase as a consequence of the change in the ELM nature (from type III to type I ELMs). On this device, it has been shown in more details that large ELMs generate a transient steepening of the ITB, which is followed by an erosion of the temperature gradients and an inwards movement of the ITB on a diffusive timescale [97]. The successful compatibility of edge MHD activities with an ITB relies on ELM penetration depth that should stay smaller then the ITB radius as discussed by [57]. Therefore on JT-60U, at low plasma current (below 1.5MA) it has been reported [57] that Type I ELMs could be combined with ITBs in steady-state fully non-inductive regime since the pedestal energy (that scales as the current) and the ELMs penetration is small enough. On the contrary, at higher plasma current (typically 1.8 MA), it has been observed that the type I ELMs lead to a shrinking of the ITBs as in the other experiments.

In this context, the successful combination of an ITBs with an H-mode requires to find a reliable access to a quiescent edge compatible with the conditions for ITBs formations. Regimes with ITBs and quiescent edge have been developed on DIII-D, JET and JT-60U using different approaches that are summarised as follow:

(i) On JET, ITB could be sustained when degrading the edge pressure pedestal with Type III ELMs activity by either controlling the ELMs activity with gas puffing, or impurity injection or by varying the edge current density. This approach does not take full advantages of the edge transport barrier characteristics since it relies on the degradation of the edge pedestal that should be compensated in term of confinement by the core transport barrier.

(ii) On DIII-D, ITB could be combined with a specific edge regime without ELMs, in the so-called QDB mode that stands for Quiescent Double Barrier [20]. This regime was observed in a wide range of plasmas configurations in terms of edge triangularity and edge safety factor but with low density/high temperature at the pedestal and with counter neutral beams.

(iii) On JT-60U, disappearance of type I ELMs activity (grassy ELMs) in high β_p regimes with β_p in the range of 2 at high q_{95} has lead to the development of non-inductive regime with ITB at large radius while keeping high edge pressure pedestal (Figure 18). Grassy or small ELM regimes, with similar pedestal characteristic of Type I ELMs have also been developed on JET at high β_p [92] and on ASDEX-U [102] but without being combined with an ITB.

Other promising approaches to mitigate the ELMs activity to reach a quiescent H-mode edge by either using external magnetic configuration to ergodize the magnetic field lines [25] or by triggering artificial ELMs with pellet injection [64], have not yet been applied in advanced tokamak regimes with ITBs. Further experimental effort should be devoted in various devices in view of defining the operational window requires for the simultaneous formation of quiescent edge with ITBs.

Finally, it should be stressed that the edge conditions of ITBs regimes are usually characterised with high edge temperature and low density but at ITER-relevant collisionality. More experimental effort should be devoted to develop ITB regimes at higher (core and edge) density not only for optimizing the fusion yield (and bootstrap current) but also for achieving a better compatibility of high confinement with the power handling and plasma exhaust capabilities of the plasma facing components (high density and radiated power at the edge are simultaneously required). Pellet fuelling at the plasma edge could be used to locally increase the edge density and reduce the temperature. A key question is to determine the edge conditions compatible with good core confinement and the power handling capabilities and plasma exhaust of the divertor in steady-state advanced regimes. Quantitative answer to this open question will give a robust scientific basis for a reliable extrapolation of ITBs regimes on ITER since in the current design a beryllium first wall with tungsten brushes at the divertor entrance and CFC (carbon fibre reinforced carbon) tiles at the divertor strike points are foreseen. This means that, in addition to the exhaust and power handling requirements, high-Z impurities have to be kept at sufficiently low concentrations that may impose stringent limits to the edge plasma parameters. In this context, JET will install in 2008 a new Beryllium wall in the main chamber and tungsten divertor (with a possible option in the present project of using CFC tiles at the divertor strike points). Therefore, an important and challenging experimental effort will be devoted to develop ITBs regimes on JET with edge parameters that will be compatible with the proposed modifications to the plasma facing components including material changes to the first wall and divertor. This should provide crucial and unique information for the future of advanced regimes in ITER relevant conditions.

CONCLUSION AND DISCUSSION

By reviewing the recent progress made in understanding the underlying physics of regimes with improved core confinement (with internal transport barrier), one could already confirm that this is a very active field of research and that important progress (on both the experimental and modelling sides) have been made in various devices. The results achieved so far have been reviewed in this paper in the light of the critical physics issues relevant to the extrapolation of ITB regimes to next-step experiments, such as ITER. Indeed, it has been recognised that in next step devices the domain of operation of advanced regimes in terms of physics parameters will differ from the present mode of operation. Advanced regimes will operate simultaneously with a dominant fraction of bootstrap current at high fusion performance with β_N values approaching MHD stability limits, at high density and T_i/T_e~1 with low torque injection in conditions of core electron heating and self-heating by fusion born alpha particles. Therefore, advanced regimes will operate in a different range of dimensionless plasma parameters that govern basic plasmas physics processes such as the normalised Larmor radius, $\rho*$, collisionality, ν_e*, Mach number, M_Φ, and the ratio of ion to electron temperature, T_i/T_e. In particular, it will require operating the plasmas with simultaneously low values of $\rho*$, ν_e*, M_Φ and with T_i/T_e~1 at high β_N. To better answer the question of the extrapolation of advanced regimes in next step devices, the progress achieved so far have been analysed by addressing the following critical physics issues:

(i) conditions for ITB formation and existence of a power threshold
(ii) ITB sustainment at T_i~T_e, with low toroidal torque injection at high density and low impurity concentration
(iii) control of confinement for sustaining wide ITBs that encompass a large volume at high β_N
(iv) real time profile control with high bootstrap current and large fraction of alpha-heating
(v) compatibility of edge and core transport barriers while respecting constrains imposed by plasma facing components

It has been shown that the present experimental results provide some valuable and promising answers to these critical issues. Indeed, recent progress (typically in the last two years) have been made in different devices and could be summarised as follow:

(1) broad ITBs have been formed and sustained by tailoring the q-profile (DIII-D, JET, JT-60U);
(2) plasmas with broad ITBs have been sustained at high-β_N values reaching up to 4 (DIII-D);
(3) identity experiments have been carried out in the ITB regimes between ASDEX-Upgrade and JET;
(4) ITBs plasmas have been sustained with a dominant fraction of bootstrap current (I_{boot}/I_p>50%) for more than one resistive time (DIII-D, JT-60U, TCV);
(5) in fully non-inductive current drive regimes plasma oscillations related to the non-linear coupling between heat transport, q-profile and non-inductive sources have been observed and characterised in details (DIII-D, Tore Supra);
(6) real time control techniques have been developed to control not only global quantities but also radial profiles such as the q-profile or/and temperatures profiles (DIII-D, JET, JT-60U);

(7) ITBs have been sustained with low torque injection with dominant RF heating schemes (Alcator-C mode, FT-U, T-10, TCV, Tore Supra) and in some conditions ITBs have been sustained at T_i~T_e by varying the ratio of ion to electron heating (ASDEX-U, DIII-D, JET, JT-60U);

(8) core impurities transport has been characterised in details showing that neo-classical accumulation of high-Z elements could be avoided providing that the density gradient is controlled (DIII-D, JET, JT-60U); it has been also shown that Helium is not accumulating and could be pumped (JET, JT-60U);

(9) H-mode plasmas with high pressure at the pedestal edge with grassy ELMs or quiescent edge have been successfully combined with ITBs conditions (DIII-D, JT-60U).

Finally, based on these important and promising results one could propose research direction where more experimental and modelling efforts could be pursued in the coming years. Indeed, additional efforts should be devoted towards the realisation of integrated advanced tokamaks scenarios where the progress made mainly in an independent manner along the various lines of researches just summarised above could be further combined. In this context, activities where further experimental and modelling effort will provide valuable information for a reliable extrapolation of ITBs regimes in view of their application in next devices are listed as follow:

(1) development of ITB regimes with high fraction of bootstrap current (I_{boot}/I_p>50%) without compromising in terms of fusion performances;

(2) development of profile control techniques in bootstrap dominated regimes and at high β_N where the alpha-particle heating source could already be simulated experimentally using central electron heating;

(3) development of techniques to control the density profile in order to avoid impurity accumulation while optimising the fusion performances, bootstrap current and ensuring the compatibility with the wall/divertor requirements;

(4) assessment of the optimum q-profile for improved MHD stability and confinement;

(5) continue the basic physics understanding of turbulence stabilisation mechanisms by performing identity and similarity experiments between various devices;

(6) development of high fusion yield regimes with a larger fraction of electron heating to operate at T_i/T_e closer to unity while simultaneously keeping low values of M_ϕ, ρ^* and ν_*;

(7) achievement of a better compatibility of high confinement regimes with the power handling and plasma exhaust constrains imposed by the future plasma facing components (eg. Beryllium walls, Tungsten divertor) where high density and radiated power at the edge are simultaneously required.

Active progress along these lines of researches will facilitate greatly the experimental development of advanced tokamak regimes on ITER and will clarify the choice of heating (bootstrap current) and non-inductive current drive systems needed in ITER and future steady-state thermonuclear reactor.

ACKNOWLEDGMENT

It is a great pleasure to acknowledge many fruitful discussions with JET-EFDA contributors and with members of both Transport Physics and Steady-State Operation ITPA Groups and with J. F. Artaud, Y Baranov, V. Basiuk, C. D. Challis, F. Crisanti, E. Doyle, A. Field, A. Garofalo, P. Gohil, G. Giruzzi, F. Imbeaux, N. Kirneva, T. Luce, P. Mantica, D. Moreau, V. Pericoli-Ridolfini, P. Politzer, Y. Sakamoto, O. Sauter, K. Razumova, T. Tala, A. Tuccillo and M Watkins.

REFERENCES

[1]. Andreev V.F. et al 2004 *Evolution of the transport coefficients for the transient process after ECRH switch-on/off in the T-10 Tokamak* Proc. 20th Int. Conf. on Fusion Energy (Vilamoura, 2004) (Vienna: IAEA), TH/P3-1 and http://www-pub.iaea.org/MTCD/Meetings/PDFplus/fusion-20-preprints/index.htm

[2]. Artaud J.F. et al 2005 private communication and Proc. 32nd Eur. Conf. on Plasma Physics and Controlled Fusion (Tarragona, 2005) (Geneva: European Physical Society) Vol. **29-C** P-1.035 (http://eps2005.ciemat.es/)

[3]. Aymar R., Barabaschi P. & Shimomura Y. 2002 Plasma Phys Control Fusion **44** 519

[4]. Baranov Yu. F et al 2004 Plasma Phys. Control. Fusion **46** 1181

[5]. Baranov Yu.F et al 2005 Plasma Phys. Control. Fusion **47** 975

[6]. Basiuk V. 2003 Nucl. Fusion **43** 822

[7]. Bécoulet M. et al 2003 Plasma Phys Control Fusion **45** A93

[8]. Beer M.A. et al 1997 Phys. Plasmas **4** 1792

[9]. Bourdelle C. et al 2005 Nucl. Fusion **45** 110

[10]. Budny R.V. et al 2005 this special issue of Plasma Phys. Control. Fusion

[11]. Burrell K.H. 1997 Phys. Plasmas **4** 1499

[12]. Candy J et al 2004 Phys. Plasmas **5** 1879

[13]. Casper T.A. et al 2005 this special issue of Plasma Phys. Control. Fusion

[14]. Challis C .D et al. 2002 Plasma Phys. Control. Fusion **44** 1031.

[15]. Challis C.D. 2004 Plasma Phys. Control. Fusion **46** B23

[16]. Challis C.D. & Sips G. et al 2005 private communication

[17]. Coda S. et al 2005 Phys. Plasmas **12** 56124-1

[18]. Connor J.W. et al. 2004 Nucl. Fusion **44** R1

[19]. Crombé K. et al 2005 Phys. Rev. Letters **95** 155003-1

[20]. Doyle E.J. et al 2001 Plasma Phys Control Fusion **43** A95

[21]. Doyle E.J. et al 2002 Nucl. Fusion **42** 333

[22]. Doyle E.J. et al 2005 this special issue of Plasma Phys. Control. Fusion

[23]. Dux R. et al 2004 Nucl. Fusion **44** 260
[24]. Eriksson L.G. et al 2002 Phys. Rev Letters **88** 145001-1
[25]. Evans T.E. et al 2005 Nucl. Fusion **45** 595
[26]. Fable E et al Proc. 32nd Eur. Conf. on Plasma Physics and Controlled Fusion (Tarragona, 2005) (Geneva: European Physical Society) Vol. **29-C** P-1.051 (http://eps2005.ciemat.es/)
[27]. Field A. et al 2004 IAEA *Core Heat Transport in the MAST Spherical Tokamak* Proc. 20th Int. Conf. on Fusion Energy (Vilamoura, 2004) (Vienna: IAEA), EX/P2-11 and http://www-pub.iaea.org/MTCD/Meetings/PDFplus/fusion-20-preprints/index.htm
[28]. Fiore C.L. et al 2004 Plasma Phys Control Fusion **46** B281
[29]. Frigione D. et al., 2003
[30]. Proc. 30th Eur. Conf. on Plasma Physics and Controlled Fusion (St Petersburg, 2003) (Geneva: European Physical Society) Vol. **27A** P-2.91 (http://eps2003.ioffe.ru/)
[31]. Fujita et al 2001 Phys. Rev. Letters **87** 85001-1
[32]. Fujita et al 2004 Plasma Phys. Control. Fusion **46** A35
[33]. Garbet X et al 2001 Phys. Plasmas **8** 2793
[34]. Garbet X et al 2004 Plasma Phys. Control. Fusion **46** B557
[35]. Garofalo A.M. et al Proc. 32nd Eur. Conf. on Plasma Physics and Controlled Fusion (Tarragona, 2005) (Geneva: European Physical Society) Vol. **29-C** O-4.006 (http://eps2005.ciemat.es/) and Garofalo A.M. et al 2005 submitted to Phys. of Plasmas
[36]. Giruzzi G. et al 2003 Phys. Rev Letters **91** 135001-1
[37]. Giruzzi G. on behalf of the Tore Supra Team 2005 Plasma Phys Control Fusion **47** B93
[38]. Gohil P. 2002 Plasma Phys Control Fusion **44** A37
[39]. Gohil P. et al. 2003 Nucl. Fusion **43** 708
[40]. Gohil P. et al 2005 this special issue of Plasma Phys. Control. Fusion
[41]. Gormezano C. 1999 Plasma Phys. Control. Fusion **41** B367
[42]. Green B. J. et al. 2003 Plasma Phys. Control. Fusion **45** 687
[43]. Greenfield C.M. et al 2000 Proc. 27th Eur. Conf. on Plasma Physics and Controlled Fusion (Budapest, 2000) (Geneva: European Physical Society) Vol. **24-B** p 544
[44]. Günter S. et al 2000 Phys. Rev Letter **84** 3097
[45]. Hayashi N et al 2005 this special issue of Plasma Phys. Control. Fusion
[46]. Henderson M.A. et al 2004 Phys. Rev Letter **93** 215001-1
[47]. Hoang G.T. et al 2000 Phys. Rev Letter **84** 4593
[48]. Hogeweij G.M.D. et al 1998 Nucl. Fusion **38** 1881
[49]. Hogeweij G.M.D. et al 2001 Plasma Phys. Control. Fusion **44** 1155
[50]. Ide S. et al 2004 Nucl. Fusion **44** 87
[51]. Imbeaux F. et al 2005 submitted to Phys. Rev Letters ITER Physics Basis 1999 Nucl. Fusion **39** 2137
[52]. Jenko F. et al 2001 Phys. Plasmas 8 4096

[53]. Joffrin E. et al 2003 Nucl. Fusion **43** 1167
[54]. Jones T.T.C. et al. 2001 Proc. 28th Eur. Conf. on Plasma Physics and Controlled Fusion (Funchal, 2001) (Geneva: European Physical Society) Vol. **25A** P1197
[55]. Kamada Y. et al 2000 Plasma Phys Control Fusion **42** A247
[56]. Kamada Y. et al 2002 Fusion Science & Technology **42** 185
[57]. Kamada Y. et al 2005 this special issue of Plasma Phys. Control. Fusion
[58]. Kikuchi M. 1990 Nucl. Fusion **30** 265
[59]. Kinsey J.E. et al 2001 Phys. Review Letters **86** 814
[60]. Kirneva N.A. et al 2005 Plasma Phys Control. Fusion **47** 1787
[61]. Kishimoto H., Ishida S., Kikuchi M. and Ninomiya H. 2005 Nucl. Fusion **45** 986
[62]. Koide Y. et al 1994 Phys. Rev. Lett. **72** 3662
[63]. Laborde L et al 2005 Plasma Phys Control. Fusion **47** 155
[64]. Lang P.T. et al 2005 Nucl. Fusion **45** 502
[65]. Lebedev V.B. and Diamond P.H. 1997 Phys. Plasmas **4** 2393
[66]. Leonov V.M. and Zhogolev V.E. 2005 Plasma Phys. Control. Fusion **47** 903
[67]. Lin-Liu Y.R. and Stambaugh R 2004 Nucl. Fusion **44** 548
[68]. Litaudon X. 1998 Plasma Phys. Control. Fusion **40** A251
[69]. Litaudon X. et al 2001 Plasma Phys. Control. Fusion **43** 677
[70]. Litaudon X. et al 2004 Plasma Phys. Control. Fusion **46** A19
[71]. Litaudon X. et al. 2003 Nucl. Fusion **43** 565
[72]. Luce T. C. et al 2005 Fusion Science & Technology **48** 1212
[73]. Mantica P. et al 2005 submitted to Phys. Rev. Letters
[74]. Mazon D. et al 2002 Plasma Phys Control. Fusion **44** 1087
[75]. McDonald D. et al 2003 Plasma Phys. Control. Fusion **46** A215
[76]. Moreau D. et al 2003 Nucl. Fusion **43** 870
[77]. Nazikian R. et al 2005 Phys. Review Letters **94** 135002-1
[78]. Neu et al 2002 Plasma Phys. Control. Fusion **44** 811
[79]. Neutdatchin S.V. et al 2004 Nucl. Fusion **44** 945
[80]. Neutdatchin S.V et al 2005 this special issue of Plasma Phys. Control. Fusion
[81]. Parail V.V. et al 1999 Nucl. Fusion **39** 429
[82]. Peeters A.G. et al 2002 Nucl. Fusion **42** 1376
[83]. Pericoli-Ridolfini V. et al 2005 Plasma Phys. Control. Fusion 47 B285
[84]. Peysson & Tore Supra Team 2001 Nucl. Fusion **41** 1703
[85]. Petty C.C. et al 2004 Physics of Plasmas **11** 2514
[86]. Polevoi A.R. et al 2004 Possibility of Q>5 stable, steady-state operation in ITER with moderate β_N and H-factor Proc. 19th Int. Conf. on Fusion Energy (Lyon, France 2002) (Vienna: IAEA), CD-ROM file IAEA CT-/P-08 and http://www.iaea.org/programmes/ripc/physics/fec2002/html/fec2002.htm/

[87]. Politzer P.A. et al 2005 Nucl. Fusion **45** 417
[88]. Razumova K.A. *et al* 2002 Role of *q* profile in the transport barriers formation on the T-10 Tokamak *Proc. 19th Int. Conf. on Fusion Energy (Lyon, 2002)* (Vienna: IAEA), CD-ROM file IAEA-CN-94/ EX/ P3-03 and http://www.iaea.org/programmes/ripc/physics/fec2002/html/fec2002.htm
[89]. Razumova K.A. et al 2004 Nucl. Fusion **44** 1067
[90]. Rebut P.H., Boucher D., Gormezano G., Keen B.E. and Watkins M.L. 1993 Plasma Phys. Control. Fusion **35** A3
[91]. Rice J.E. et al 2003 Nuc Fusion **43** 781
[92]. Saibene G. et al 2005 Nucl. Fusion **45** 297
[93]. Sakamoto Y. et al 2001 Nucl. Fusion **41** 865
[94]. Sakamoto Y. et al 2004 Nucl. Fusion **44** 876
[95]. Sakamoto Y. et al 2005a Nucl. Fusion **45** 574
[96]. Sakamoto Y. et al 2005b this special issue of Plasma Phys. Control. Fusion
[97]. Sarazin Y. et al 2002 Plasma Phys Control Fusion **44** 2445
[98]. Sauter O. et al 2005 Phys. Rev Letter **84** 105002-1
[99]. Shimada M. et al 2004 Nucl. Fusion **44** 350
[100]. Shirai H. et al 2000 Plasma Phys. Control. Fusion **42** A109
[101]. Sips A.C.C. et al 2004 *Study of Advanced tokamak performance using the international tokamak physics activity database* Proc. 20th Int. Conf. on Fusion Energy (Vilamoura, 2004) (Vienna: IAEA), CD-ROM file IAEA IT/ P3-36 and http://www-pub.iaea.org/MTCD/Meetings/PDFplus/fusion-20-preprints/index.htm
[102]. Stober J. et al 2001 Nucl. Fusion **41** 1123
[103]. Suzuki T. et al 2004 *Steady State High β_N Discharges and Real-Time Control of Current Profile in JT-60U* Proc. 20th Int. Conf. on Fusion Energy (Vilamoura, Portugal 2004) (Vienna: IAEA) CD-ROM file IAEA EX/1-3 and http://www-pub.iaea.org/MTCD/Meetings/PDFplus/fusion-20-preprints/index.htm
[104]. Synakowski E.J. et al 1997 Phys. Rev. Letters **78** 2972
[105]. Takenaga et al 2004 Proc. 20th Int. Conf. on Fusion Energy (Vilamoura, Portugal 2004) (Vienna: IAEA), CD-ROM file IAEA EX/1-3 and http://www-pub.iaea.org/MTCD/Meetings/PDFplus/fusion-20-preprints/index.htm
[106]. Tala T. J. J. et al 2001 Plasma Phys. Control. Fusion
[107]. Tala T. J. J. et al 2004 *Fully predictive transport simulations of ITB plasmas in JET,JT-60U and DIII-D* Proc. 20th Int. Conf. on Fusion Energy (Vilamoura, Portugal 2004) (Vienna: IAEA), CD-ROM file IAEA TH/P2-9 and http://www-pub.iaea.org/MTCD/Meetings/PDFplus/fusion-20-preprints/index.htm
[108]. Tala T. J. J. et al 2005 Nucl. Fusion **45** 1027

[109]. Tala T.J.J. Proc. 32nd Eur. Conf. on Plasma Physics and Controlled Fusion (Tarragona, 2005) (Geneva: European Physical Society) Vol. **29-C** P-4-044 (http://eps2005.ciemat.es/)
[110]. Taylor T. S., 1997 Plasma Phys. Control. Fusion **39** B47
[111]. Tresset et al 2002 Nucl. Fusion **42** 520
[112]. Tuccillo A. A. et al 2005a Plasma Phys. Control. Fusion **47** B363
[113]. Tuccillo A. A. et al 2005b to be published in Nucl. Fusion
[114]. Weiland J. et al 2000 Collective modes in inhomogeneous plasmas, Institute of Physics Publishing, Bristol
[115]. Wolf R C 2003a Plasma Phys. Control. Fusion **45** R1
[116]. Wolf R. C. et al 2003b Plasma Phys. Control. Fusion **45** 1757
[117]. Zastrow K-D et al 2004 Plasma Phys. Control. Fusion **46** B255
[118]. Zastrow K-D et al 2005 Nucl. Fusion **45** 163

Table 1.

Discharge parameters for ITB identity experiments between ASDEX-U and JET [16].
The parameters have been selected just prior the ITB formation.

Parameters	AUG Pulse No: 16147 (t = 0.7s)	JET Pulse No: 62175 (t=2.5s)
R [m] /a [m]	1.6/0.5	2.9/0.95
$\kappa/\langle\delta\rangle$	1.8/0.24	1.7/0.22
B_o [T]	3	1.8
I_p [MA]	0.78	0.81
q_{95}	6.8	7.6
$\langle n_e\rangle$ [$10^{19}m^{-3}$]	2.3	1.1
$\langle T_e\rangle$ [keV]	1.2	0.6
ρ*	4.5×10^{-3}	$3.0 - 3.6 \times 10^{-3}$
ν_e*	0.25	0.27 – 0.7

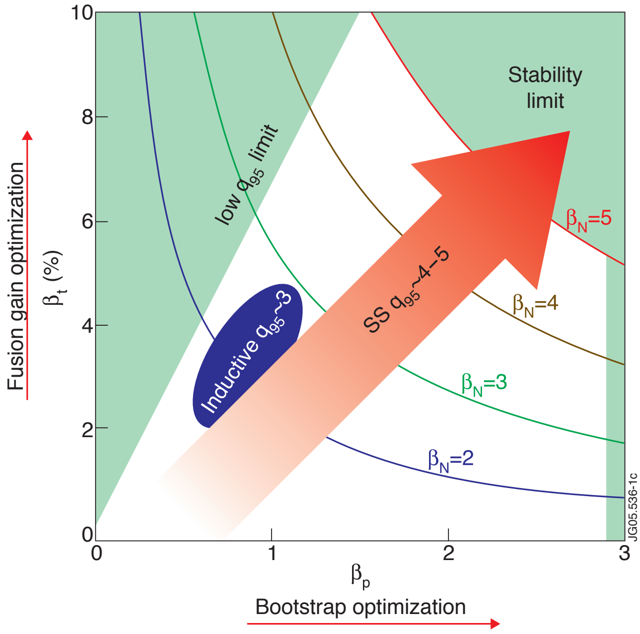

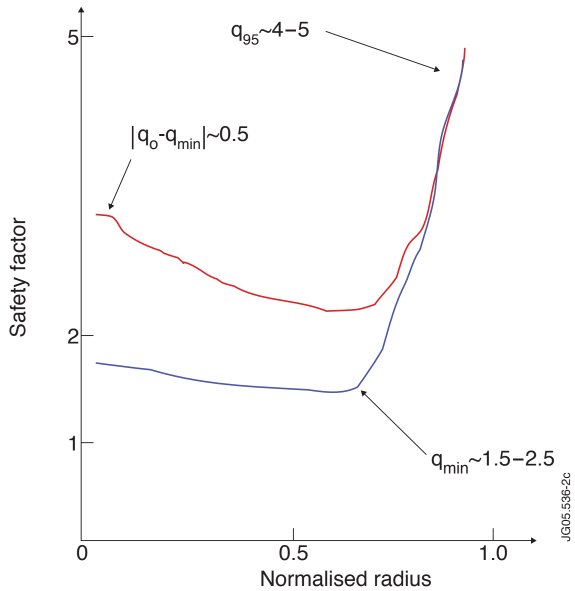

Figure 1: Toroidal beta, β_t, versus poloidal beta, β_p, assuming κ=2 from the simplified formula (3). The schematic domains of tokamak operation for inductive (q_{95}~3) and steady-state (SS) regimes (q_{95}~4-5) are both shown in this (β_t, β_p plane. The low q and high β_N limits are drawn in a schematic manner. The high β_N limit depends on plasma shaping, profile, wall stabilisation and could be further optimised depending on the reactor design for continuous operation.

Figure 2: Typical range of q-profile for steady-state fully non-inductive current drive operation as proposed by the ITPA group on Steady-State Operation.

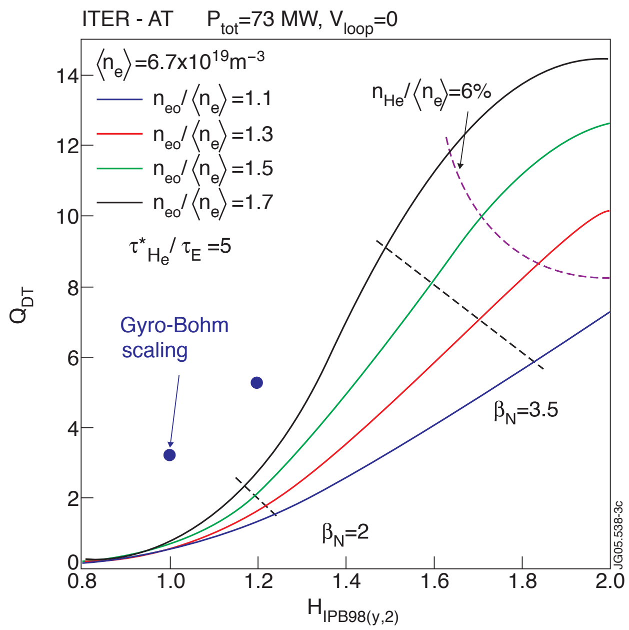

Figure 3: ITER zero loop voltage operation (V_{loop}=0): Fusion gain, $Q_{DT,}$ versus the enhanced confinement $H_{IPB98(y,2)}$ factor assuming ITER geometric parameters and with 73MW of applied power (33MW of neutral beam injection, 20MW of ICRH and 20MW of LHCD).

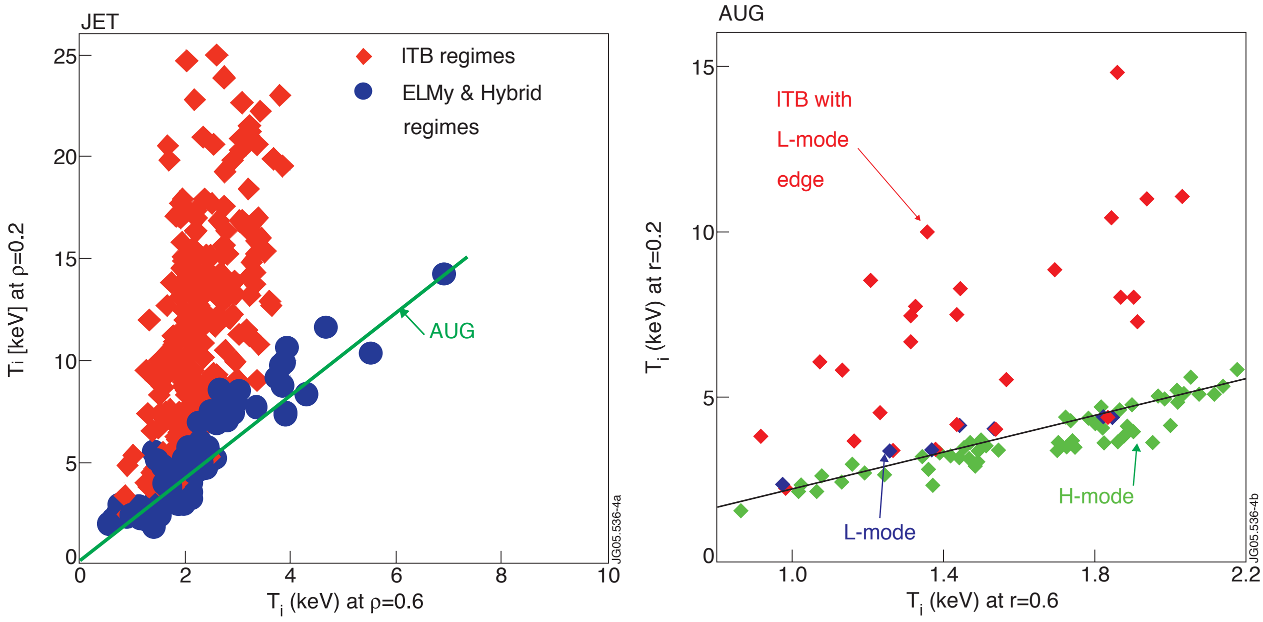

Figure 4: (left) Core ion temperature against temperature at r/a=0.6 on JET and (right) on ASDEX-U for various plasma regimes with and without ITB [Figure 4 (right) is reproduced from Peeters A G et al 2002 Nucl. Fusion 42 1376].

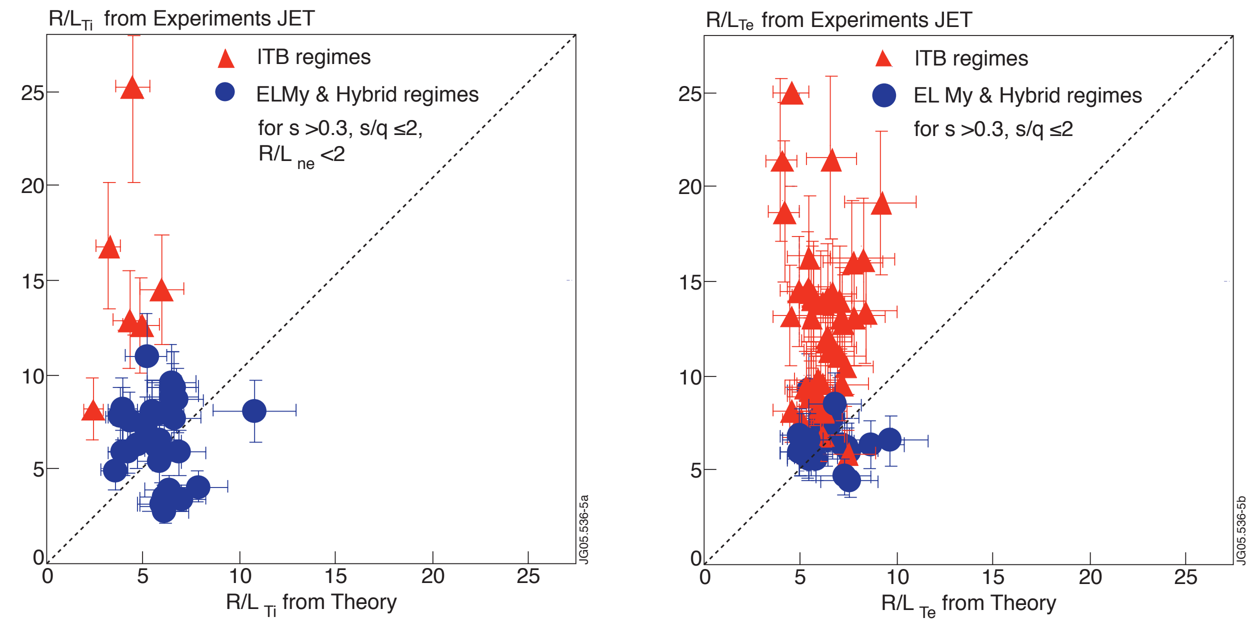

Figure 5: JET normalised local temperature gradient, R/L_{Ti} (left) and R/L_{Te} (right) against the expected theoretical scaling. The theoretical scaling used for the electron is $R/L_{Te} = (1 + Z_{eff} T_e/T_i)(1.33 + 1.91\,|s|/q)$ and for the ion $R/L_{Ti} = (1 + T_i/T_e)(1.1 + 1.4\,|s| + 1.9\,|s|/q)$ where s is the local magnetic shear. All the local quantities have been estimated at mid plasma radius and selecting data where s>0.3 and s/q ≤ 2 corresponding to the range of validity for the theoretical scaling.

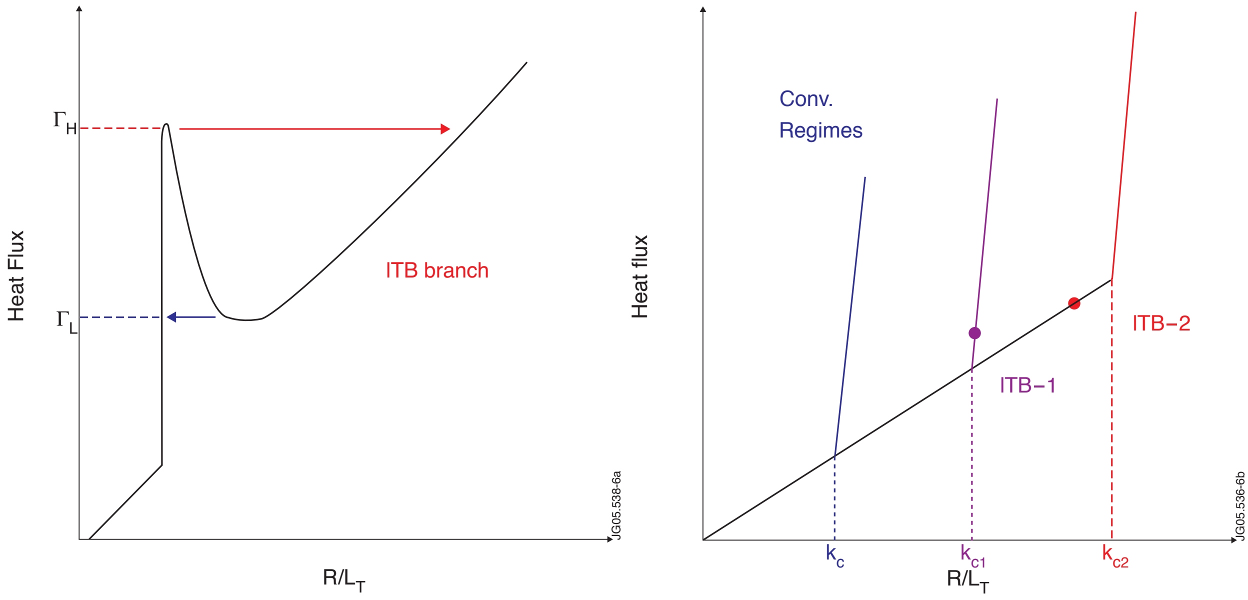

Figure 6: (left) a first order flux-gradient schematic diagram showing a bifurcation between an L-mode and ITB branch when the heat flux exceeds a certain threshold; (right) a second order flux gradient schematic diagram with two cases for the transition towards an ITB regime.

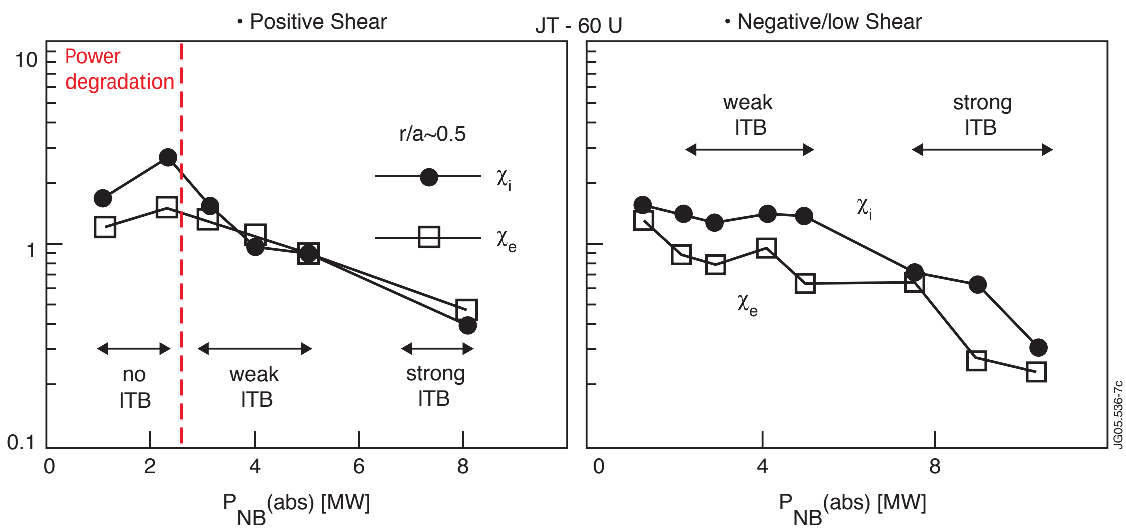

Figure 7: Dependence of thermal transport coefficients (χ_e and χ_i) on heat flux in positive (left) and negative (right) magnetic shear plasmas [reproduced from Sakamoto Y. et al 2004 Nuc. Fusion 44 876].

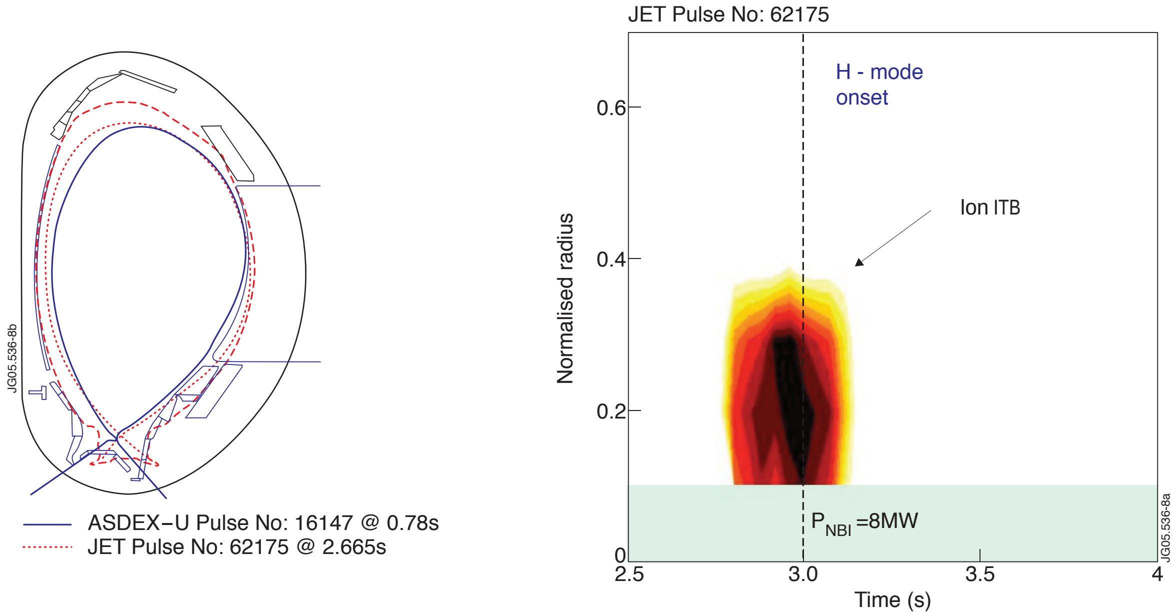

Figure 8: (left) Plasma shapes for ITB identity experiments between ASDEX-U (full line) and JET (dashed line). In this graph, the JET magnetic configuration (dashed line) has been superimposed to the ASDEX-U one by applying a scaling factor. (right) Time evolution of the radial location (in normalised radius) of the ion ITB in JET identity experiments with ASDEX-U (JET #62175) [Challis C.D. & Sips G. et al 2005 private communication].

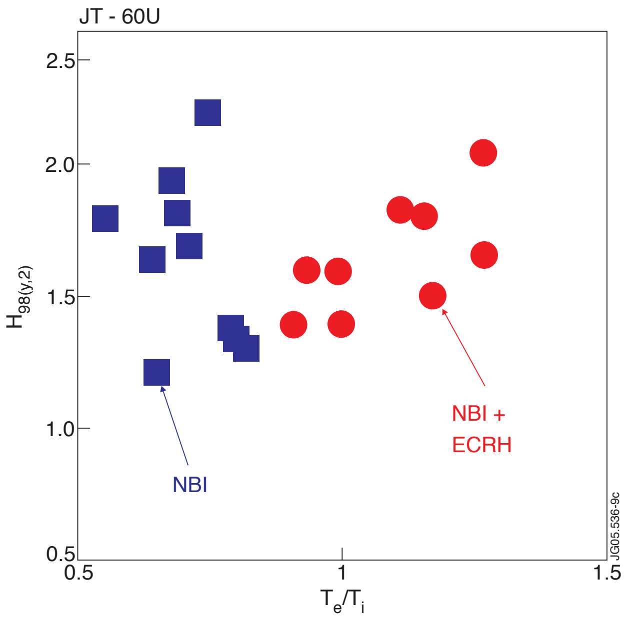

Figure 9: JT-60U Enhanced confinement factor, $H_{IPB98(y,2)}$, against the ratio of T_e/T_i in ITB experiments with either NBI heating (full squares) or with NBI heating combined with ECRH once the ITBs have formed (full circles) [reproduced from Ide S. et al 2004 Nucl. Fusion 44 87].

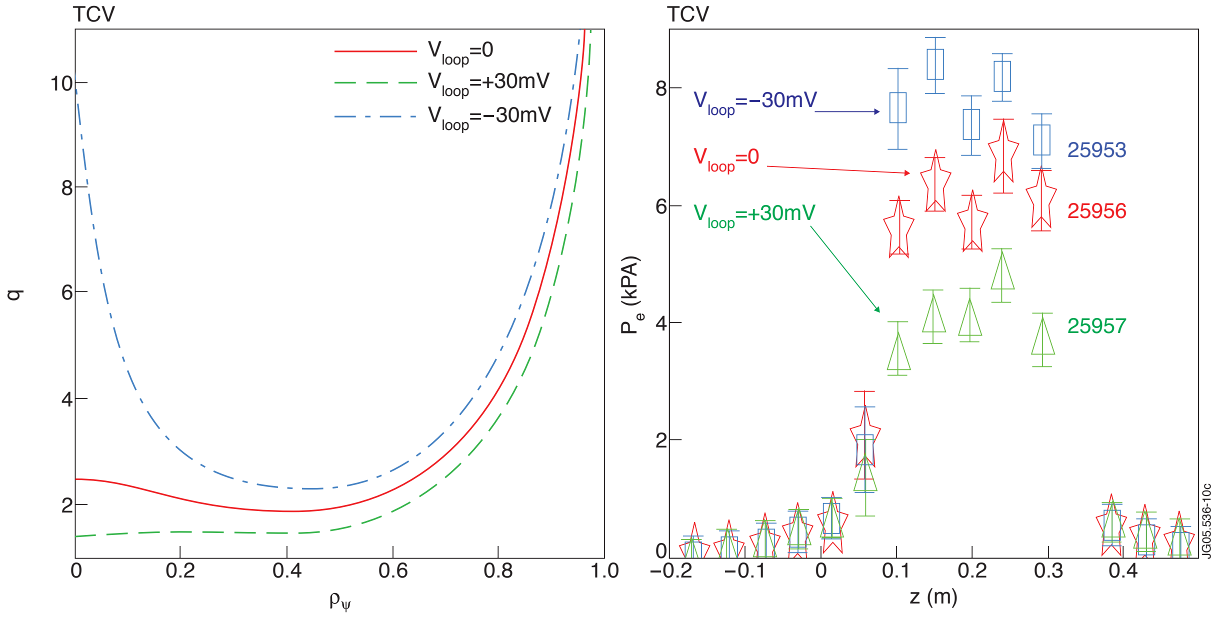

Figure 10: TCV (left) Scan of q-profile by varying the applied loop voltage (V_{loop}=0, V_{loop}=±30mV) and (right) the corresponding electron pressure profiles [reproduced from Sauter et al 2005 Phys. Rev Letter 84 105002-1]

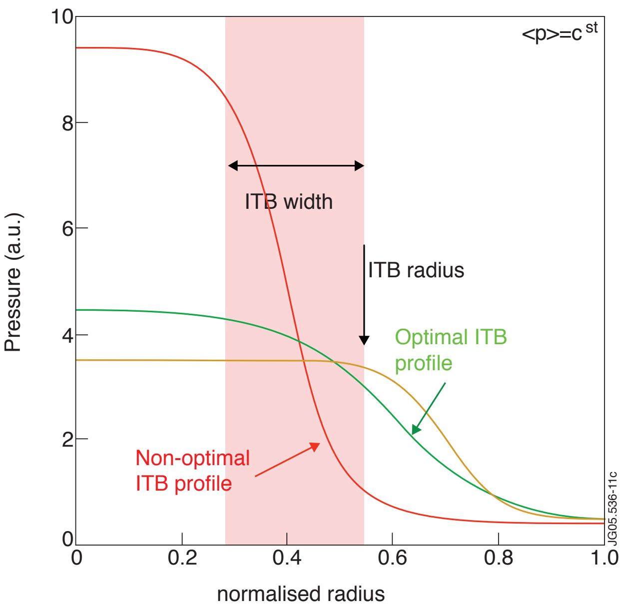

Figure 11: Pressure profiles representing in schematic way different cases of ITB profiles (optimal and non-optimal ITB profiles) at constant volume averaged pressure.

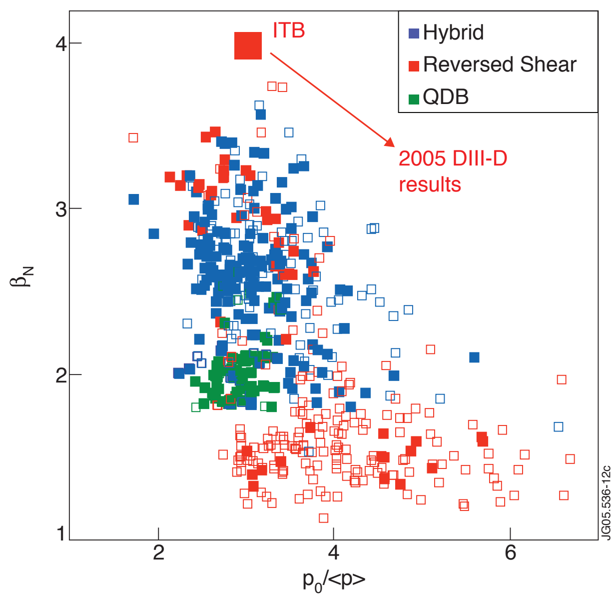

Figure 12: β_N versus the pressure peaking factor, P_o/·PÒ, for different advanced regimes from the ITPA ITB 0-D database [ASDEX Upgrade, FT-U, DIII-D, JET, JT-60U, TCV and Tore Supra data]. The closed symbols correspond to the stationary results characterised by a high performance phase longer than 10 × τ_E whereas the transient results have open symbols. Reproduced from Sips et al 2004 Proc. 20th Int. Conf. on Fusion Energy (Vilamoura, Portugal 2004) but adding the new experimental result obtained in DIII-D at β_N~4 with P_o/·PÒ ranging between 2.5 and 3.2 (Doyle E.J. et al 2005 … Garofalo A.M. et al 2005).

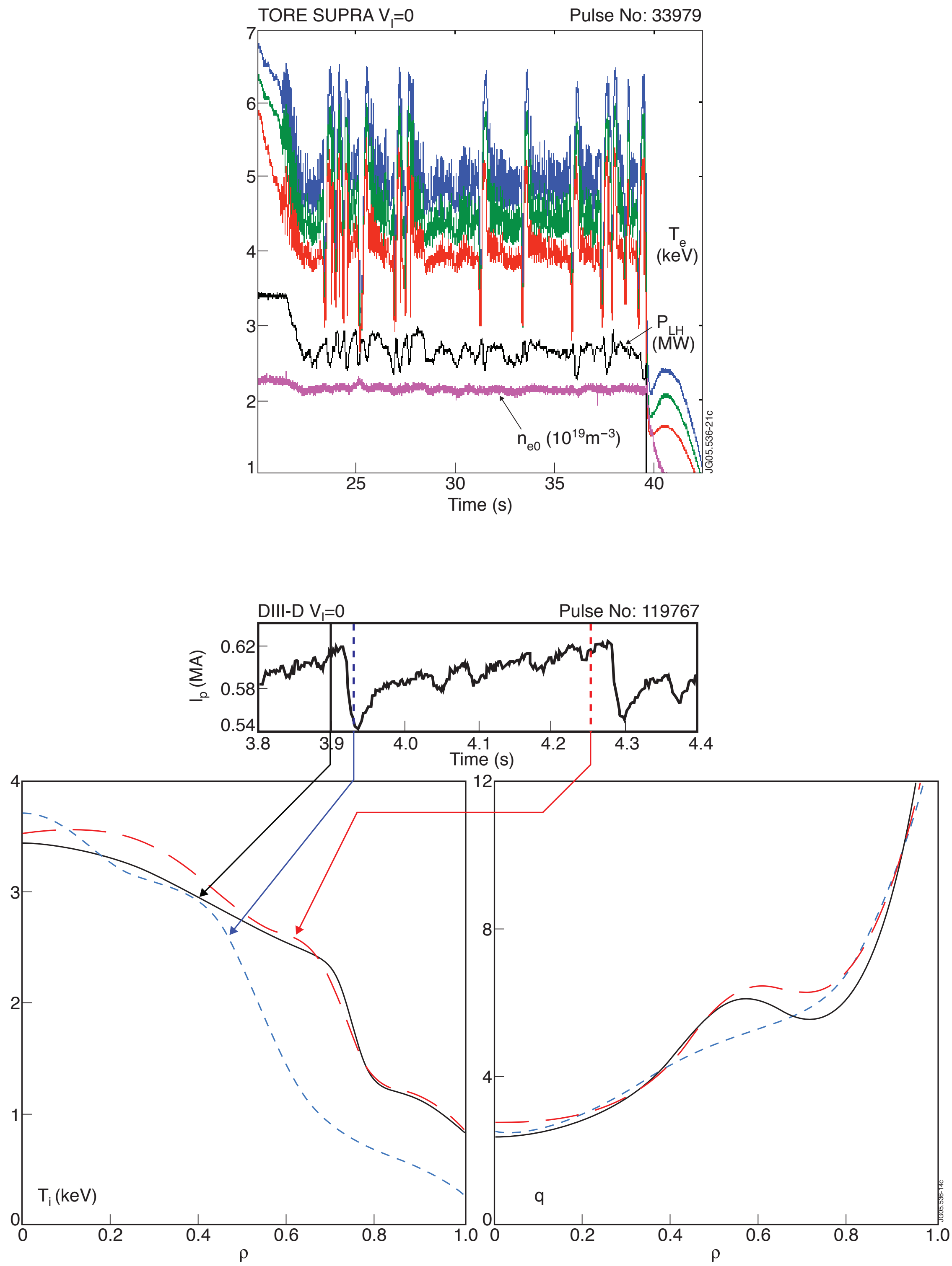

Figure 13:(left) Tore Supra full current drive operation sustained with LHCD; Time evolution of T_e in the plasma core (r/a<0.2), LH power (P_{LH}) and central electron density (n_{eo}) showing on the T_e evolution that the plasma could behave as a two-cycles non-linear oscillators with intermittent transitions from small periodic oscillations to giant oscillations [Imbeaux et al 2005, Giruzzi et al 2005]. (right) DIII-D high bootstrap full current drive operation. Expanded view of a single cycle of the ITB relaxation oscillation: plasma current and profiles of the ion temperature and safety factor just before the ITB collapse, just after the collapse and just before the next ITB collapse [Reproduced from Politzer P.A. et al 2005 Nucl. Fusion 45 417].

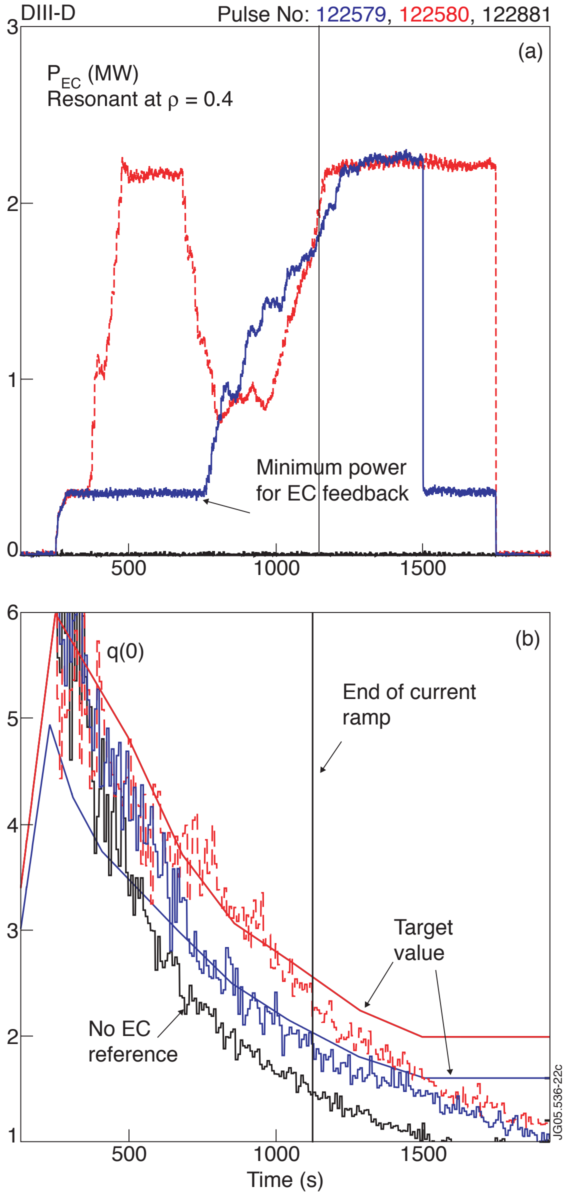

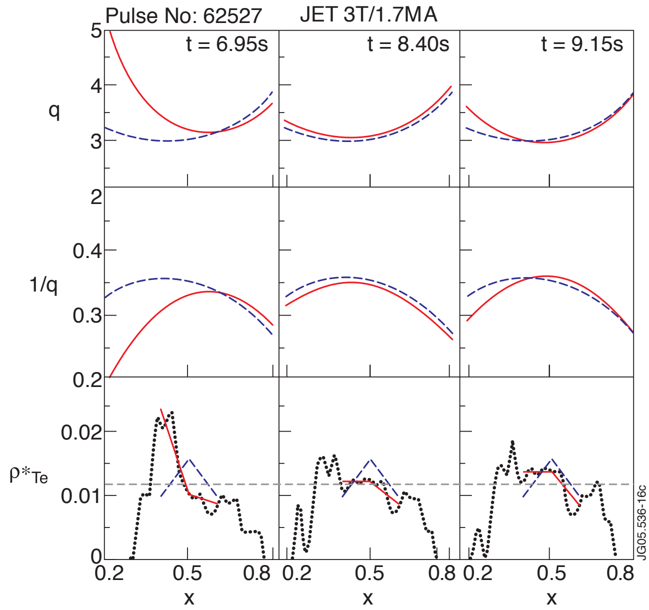

Figure 14: (left) DIII-D real time control of q_o evolution in L-mode using off-axis ECRH power at a normalised radius of 0.4; (a, top) applied ECRH power for two L-mode discharges, (b, bottom) closed loop control of q_o to the pre-set target values for the two corresponding discharges and for the reference case without ECRH [reproduced from Gohil et al 2005 this special issue of Plasma Phys. Control. Fusion]; (right) JET simultaneous real time control of q and T_e profile with LHCD, NBI and ICRH powers. Measured (solid lines) and target (dashed lines) profiles at various times during the control phase for the safety factor (q), its inverse τ=1/q and the normalised temperature gradient, ρ^*_{Te} as defined by Tresset et al (2002) For ρ^*_{Te} the original profile has also been added (dotted) [reproduced from Laborde L. et al 2005 Plasma Physic and Control Fusion 47 155].

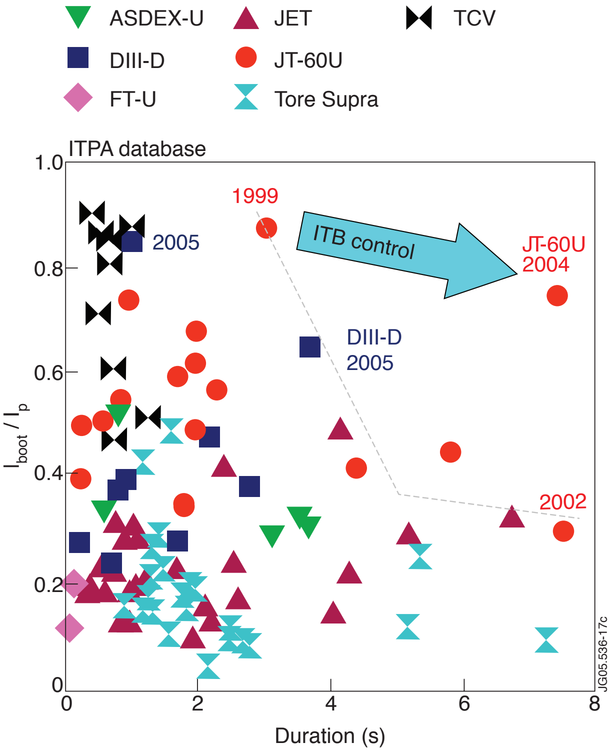

Figure 15: Bootstrap current fraction against duration of the sustainement of the high performance phase. The experimental points are from the multi-machine ITPA ITB global database as published in Litaudon et al (2004) but including the recent results published in 2005 by DIII-D (Politzer et al 2005) and JT-60U (Sakamoto et al 2005).

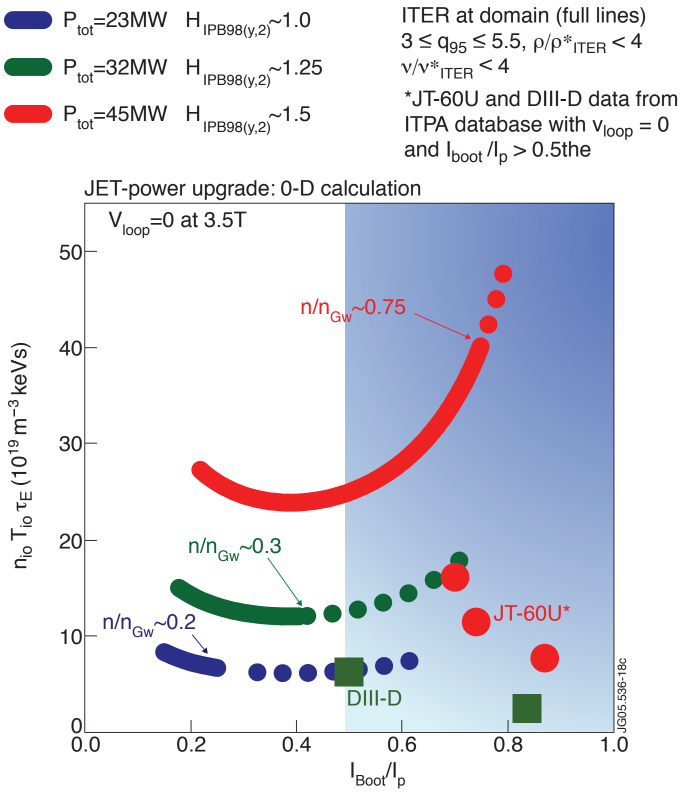

Figure 16:"JET-power upgrade: Calculated fusion triple product $n_{io}xT_{io} \times \tau_E$ versus I_{boot}/I_p for various power level in fully non-inductive current drive conditions combining LHCD, Neutral Beam Current Drive with ICRH heating. The experimental points from JT-60U and DIII-D have been selected from the ITPA ITB database with the simultaneous conditions of V_{loop}=0 and I_{boot}/I_p>50% (there is no JET data that presently meets simultaneously these two conditions).

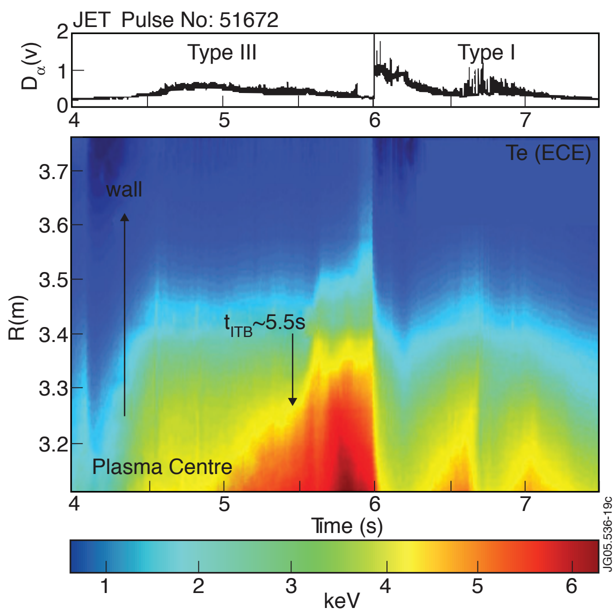

Figure 17: JET- Time evolution of divertor Dα signal (top) and electron temperature versus time and major radius showing the formation of the ITB with a hot core at t_{ITB}~4.5s and its collapse after the change in the ELM nature (BÈcoulet M. et al 2003 Plasma Phys Control Fusion 45 A93).

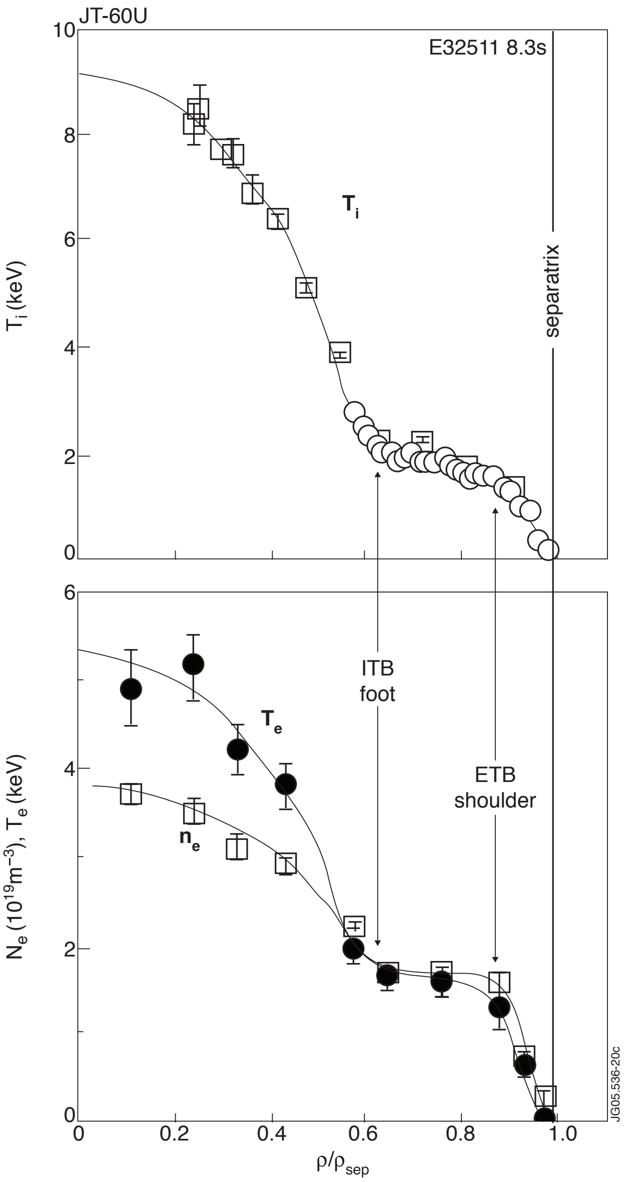

Figure 18: JT-60U- Kinetic profiles of T_i, T_e and n_e in a high-β_p H mode discharge where ITB and edge transport barrier with grassy ELMs with high pressure pedestal have been successfully combined [reproduced from Kamada Y. et al 2000 Plasma Phys Control Fusion 42 A247].